THE EFFECTS OF PRESSURE ON THE MECHANICAL PROPERTIES AND MICROSTRUCTURE OF DIE CAST ALUMINUM ALLOYS

By

Nnamdi Kenneth OBIEKEA, B.Eng (Mech)

(M.Sc/ENG/2824/2009-2010)

Department of Mechanical Engineering,

Ahmadu Bello University, Zaria, Nigeria.

An M.Sc Thesis submitted to the Postgraduate School, Ahmadu Bello University, Zaria, in partial fulfillment of the Requirements for the Award of Master of Science (Mechanical Engineering) in the Department of Mechanical Engineering, Ahmadu Bello University, Zaria.

February, 2013.

DECLARATION

I Nnamdi Kenneth OBIEKEA hereby declare that the work in this thesis titled **"The Effects of Pressure on the Mechanical Properties and Microstructure of Die Cast Aluminum Alloys"** is solely composed by me and that it is the result of my research work under the supervision of Prof. S.Y. and Dr. D.S. Yawas.

The information derived from literature has been duly acknowledged in the text and a list of references provided. This thesis has not been previously presented for the award of any degree or diploma at any University.

_____ _____

Nnamdi Kenneth OBIEKEA Date

CERTIFICATION

This thesis titled **"The Potentials of Carbonized Maize Stalk Particulates as Reinforcement in Polyester Matrix Composites"** meets the regulations governing the award of the degree of Master of Science of Ahmadu Bello University, and is approved for its contribution to knowledge and literary presentation.

_____ _____

Prof. S. Y. Aku Date
Chairman Supervisory Committee

_____ _____

Dr. D.S. Yawas Date
Member, Supervisory Committee

_____ _____

Dr. M. Dauda Date
Head of Department

_____ _____

Prof. Adebayo A. Joshua Date
Dean, School of Postgraduate Studies

DEDICATION

This thesis is dedicated to my parents, Mr. And Mrs. Obiekea.

ACKNOWLEDGEMENT

My profound gratitude goes to Jehovah God, the One in Whom I serve, for His strength, wisdom, understanding and guidance during the course of this research.

I am grateful for the support obtained from my supervisors, Prof. S.Y Aku and Dr. D.S Yawas all the way through this project and for bestowing constant guidance and encouragement with this thesis. The contributions of Prof S.B Hassan and Dr G.Y Pam are highly appreciated.

I also wish to acknowledge the support received from my parents Mr. and Mrs. Obiekea and also other family members for their support, patience and endurance, which have enabled me to achieve my goal.

I wish to express my gratitude to the Scientific and Equipment Development Institute (SEDI),Enugu , (Engr. Emma and Engr Ufomba) and the Science and Technology Development Research Centre (SHEDA), Abuja, (Engr Usman) and the Federal University of Science and Technology (FUTH) Minna, (Engr. B.T. Balogun) for their support, and allowing the use of casting equipment throughout the research program.

ABSTRACT

A study of the effects of pressure on microstructure and mechanical properties of die cast aluminum alloys A1350 and A380 was carried out and subsequent analysis made. Pressure was regulated at various levels in the die cast machine. Both alloys were cast into samples each under different applied pressures. The mechanical properties of both alloys were tested and microstructure analysis was done and the results for both tests were compared for both alloys. The results obtained show hardness, tensile strength, yield strength and impact strength of both alloys varied with applied pressure in the casting process. The hardness values increased with applied pressure but not too significantly from 76 to 85 HRN for A380 alloy and 77 to 86 HRN for A1350 alloy as pressure rose from 350 to 1400kg/cm^2. The yield strength of both alloys also increased with applied pressure. The impact strength and elongation both decreased with applied pressure in both alloys. Also the microstructure analysis carried out on both alloys showed structural changes in the morphologies of both alloys as some appeared granullar, lamellar, coarse e.t.c from pressure 350 to 1400kg/cm^2. Also as the pressure increased, the grains became finer and porosity decreased.

Models were developed and for all the models developed, a close relationship with the experimental results were underlying in view of the small errors generated by them and can be used to predict the experimental values of this research.

TABLE OF CONTENTS

Title		Page
Title Page		i
Declaration		ii
Certification		iii
Dedication		iv
Acknowledgements		v
Abstract		vi
Table of Contents		vii
List of Figures		x
List of Tables		xii
List of Appendices		xiii
CHAPTER 1	**INTRODUCTION**	1
1.1	Background of this study	1
1.2	Advantages of die casting	3
1.3	Aluminum A380 and A1450 alloys	4
1.4	Statement of problem	6
1.5	Present research	7
1.6	Justification of this research	7
1.7	Aims and objectives of this research	8
CHAPTER 2	**LITERATURE REVIEW**	9
2.1	Introduction	9
2.1.1	Hot chamber die casting process	10
2.1.2	Cold chamber die casting process	11
2.2	Mathematical modeling	15
2.3	Review of past work	17

CHAPTER 3 MATERIALS AND METHODS 22
3.1 Materials 22
3.1.1 Chemical composition of work piece materials 23
3.2 Equipment 25
3.2.1 Experimental procedure 26
3.3 Methodology 26
3.3.1 Pouring and melting 26
3.3.2 Pressure application 27
3.4 Description and specification of die cast machine 27
3.4.1 Operating mode 29
3.4.2 Display indication 29
3.5 Dies for experiment 29
3.5.1 Samples after casting 30
3.6 Mechanical test procedure 32
3.6.1 Tensile test 32
3.6.2 Hardness test 32
3.6.3 Impact test 33
3.7 Microstructure analysis 33
3.7.1 Etching and microscopy 33
3.7.2 Scanning electron microscope analysis 34
3.8 Regression models 34
3.8.1 Error analysis 37

CHAPTER 4 RESULTS AND DISCUSSION 38
4.1 Results 38
4.2 Discussions 45
4.2.1 Hardness 45
4.2.1.1 Regression model for hardness 45
4.2.2 Tensile strength 45
4.2.2.1 Regression model for tensile strength 46
4.2.3 Yield strength 46
4.2.3.1 Regression model for yield strength 47

4.2.4 Impact strength 47
4.2.4.1 Regression model for impact strength 48
4.3 Microstructure 48
4.3.1 Number of grains 48
4.3.1.1 Regression model for number of grains 48
4.3.2 Grain size 49
4.3.2.1 Regression model for grain size 49
4.3.3 Porosity measurement 50
4.4 Microstructure analysis 52
4.4.1 Microstructural characterization 52
4.4.2 Microstructure and micrograph of A380 samples 53
4.4.3 Microstructure and micrograph of A1350 samples 58

CHAPTER 5 CONCLUSIONS AND RECOMMENDATION 63
5.1 Conclusions 63
5.2 Recommendations for further work 65
5.3 Contribution to knowledge 65

REFERENCES 66
APPENDIXES 74

LIST OF FIGURES

Figure No	Title	Page
Figure 2.1	Hot chamber die casting cycle	10
Figure 2.2	Cold chamber die casting process	12
Figure 3.1	A1350 raw material	22
Figure 3.2	A380 raw material	22
Figure 3.3	X- ray generation schematics	24
Figure 3.4	High pressure cold chamber die casting machine	28
Figure 3.5	Samples of A1350 after casting	30
Figure 3.6	Samples of A380 after casting	31
Figure 4.1	Experimental and predicted plots of hardness vs pressure of A380	38
Figure 4.2	Experimental and predicted plots of hardness vs pressure of A1350	38
Figure 4.3	Experimental and predicted plots of tensile strength vs pressure of A380	39
Figure 4.4	Experimental and predicted plots of tensile strength vs pressure of A1350	39
Figure 4.5	Elongation vs pressure plots of A380 and A1350	40
Figure 4.6	Experimental and predicted plots of yield strength vs pressure of A380	40
Figure 4.7	Experimental and predicted plots of yield strength vs pressure of A1350	41
Figure 4.8	Experimental and predicted plots of impact strength vs pressure of A380	41
Figure 4.9	Experimental and Predicted Plots of Impact Strength vs Pressure of A1350	42
Figure 4.10	Experimental and predicted plots of number of grains vs pressure of A380	42
Figure 4.11	Experimental and predicted plots of number of grains vs pressure of A1350	43
Figure 4.12	Experimental and predicted plots of grain size vs pressure of A380	43
Figure 4.13	Experimental and predicted plots of grain size vs pressure of A1350	44
Figure 4.14	Predicted porosity vs pressure plots of A380 and A1350	44

Figure 4.15 Microstructure and micrograph of sample of A380 with injection pressure of 1400kg/cm^2 53
Figure 4.16 Microstructure and micrograph of sample of A380 with injection pressure of 1050kg/cm^2 54
Figure 4.17 Microstructure and micrograph of sample of A380 with injection pressure of 700kg/cm^2 55
Figure 4.18 Microstructure and micrograph of sample of A380 with injection pressure of 350kg/cm^2 56
Figure 4.19 Microstructure and micrograph of sample of A380 with injection pressure of 0kg/cm^2 57
Figure 4.20 Microstructure and micrograph of sample of A1350 with injection pressure of 1400kg/cm^2 58
Figure 4.21 Microstructure and micrograph of sample of A1350 with injection pressure of 1050kg/cm^2 59
Figure 4.22 Microstructure and micrograph of sample of A1350 with injection pressure of 700kg/cm^2 60
Figure 4.23 Microstructure and micrograph of sample of A1350 with injection pressure of 350kg/cm^2 61
Figure 4.24 Microstructure and micrograph of sample of A1350 with injection pressure of 0kg/cm^2 62

LIST OF TABLES

Table No	Title	Page
Table 3.1	Chemical composition of work piece materials	25
Table 3.2	Specification of die cast machine	27
Table 3.3	Input factors and their respective levels	31
Table 4.1	A380 predictor coefficient table for porosity level	50
Table 4.2	A1350 predictor coefficient table for porosity level	51
Table A1	Hardness number for A380 samples	74
Table A2	Hardness number for A1350 samples	74
Table A3	Tensile strength of A380 samples	75
Table A4	A380 predictor coefficient table for tensile strength	75
Table A5	Tensile strength of A1350 samples	76
Table A6	A1350 predictor coefficient table for tensile strength	76
Table A7	Yield strength of the A380 and A1350 samples	77
Table A8	A380 predictor coefficient table for yield strength	77
Table A9	A1350 Predictor coefficient table for yield strength	77
Table A10	Impact strength of A380 samples	78
Table A11	Impact strength of A1350 samples	78
Table A12	Number of grains for A380 samples	79
Table A13	Number of grains for A380 samples	79
Table A14	Grain sizes for A380 and A1350 samples	80
Table A15	A380 predictor coefficient table for grain size	80
Table A15	A1350 predictor coefficient table for grain size	80

LIST OF APPENDICES

Appendix Name	Title	Page
Appendix A	Tables for various experiment and modeled parameter results	74

CHAPTER ONE

INTRODUCTION

1.1 BACKGROUND

According to Richard et al, (1967), metal casting may be defined as a metal object produced by pouring molten metal into a mould containing a cavity which has the desired shape of the end product, and allowing the molten metal to solidify in the cavity. Historical data indicates that casting began around 4000 B.C. According to Taylor et al, (1959), copper was the first metal to be cast and it was used to produce bells for large cathedrals at the beginning of the 13th century. In the 14th through 16th centuries, metal casting evolved from what was an art form to the casting of engineering shaped components (Mikelonis, 1986). However, the first authenticated casting in aluminium was produced in 1876 according to Anon (1978). In the present context, die casting involves all processes that are based on use of metallic moulds (Dahle, 2002). Casting or foundry is a process of forming objects through pouring of molten metals into prepared moulds.

Casting processes are among the oldest methods for manufacturing metal goods. In most early casting processes (many of which are still used today), the mold after use is commonly collapsed in order to remove the product after solidification. The need for a permanent mold, which can be used to produce components in large quantities which are of high quality, is the obvious alternative. In the middle ages, craftsmen perfected the use of iron in the manufacture of moulds (Doehler, 1951). Moreover, the first information revolution occurred when Johannes Gutenberg developed a method to manufacture components in large quantities using a permanent metal mold. Over the centuries, the permanent metal mold processes continued to evolve. In the late 18th century, processes were developed in which metal was injected into metal dies under pressure to manufacture print type . These

developments culminated in the creation of the linotype machine for printing by Ottmar Mergenthaler in 1885 (www.en.wikipedia.org/wiki/die_casting), an automated type casting device which became the prominent type of equipment in the publishing industry.

Doehler, (1910) is credited with developing die casting for the production of metal components in large volumes. Initially, only zinc alloys were used in die casting. Demands for other metals drove the development of new die materials and process variants.

By 1915, aluminum was being die cast in large quantities. Much progress had been made in the development of die casting technologies over the last century. Developments continue to be made driving the capabilities of the process to new levels and increasing the integrity of die cast components. Cast aluminum products are in great use in various industrial sectors and more so in the aerospace industry where precision and high quality products are of utmost importance.

Most recently, pressure die cast (PDC) aluminum products have played a significant role in the renovation of historic buildings (www.webcitaion.org). The characteristics and properties of PDC aluminum as a material have led to revolutionary and innovative changes in building techniques, architectural and engineering projects. Re-melting used aluminum requires only 5 per cent of the energy needed to produce the primary metal. Thus, rather than contributing to society's growing waste problem, aluminum can be re-melted and reformed to produce a new generation of parts. Aluminum in general has always been recycled at a higher rate than most other raw materials. Given the necessary infrastructure, it is possible to recycle all aluminum in construction industry applications, for several reasons. First, there is a relatively high level of scrap aluminum available. Second, aluminum has a high scrap value, which can contribute significantly towards covering demolition costs. Finally, the infrastructure required for the collection of scrap metals is already well established and will

continue to grow on its own economic merit as it has done in the past to provide an increasingly efficient recycling system.

Nearly 40 per cent of all aluminum used today is recycled, (www.webcitaion.org), In addition all the standards that have been set for using of metal components, die cast aluminum alloys satisfy the need to the utmost. Hence, they are certified safe for use (ISO 9001). Today there is an increasing trend in the industry towards alloys that provide increased strength over traditional alloys. In order to determine whether the casting process produces a part with proper as-cast mechanical properties, microstructure prediction is required. Microstructure of metals is a useful tool in the sense that it indicates casting defects (http://business.ezinemark.com/die-casting).

1.2 ADVANTAGES OF DIE CASTING

Die casting is an efficient, economical process offering a wide range of shapes and components than any other manufacturing technique. Parts have long service life and may be designed to compliment visual appeal of the surrounding parts. The designer can gain a number of advantages and benefits by specifying die casting parts. The other advantages of die casting include:-

1.2.1 High Speed Production

Die casting provides complex shapes with close tolerances more than any other mass production process. Little or no machining is required and thousands of identical parts can be produced before additional tooling is required.

1.2.2 Dimensional Accuracy and Stability

Die casting produces parts that are durable and dimensionally stable, while maintaining close tolerances. They are also heat resistant.

1.2.3 Strength and Weight

Die cast parts are stronger than plastic injection molded parts having the same dimensions .Thin walled castings are stronger and lighter than those possible with other casting methods. Die cast products do not require separate parts to be welded or fastened together and the strength is that of the alloy which is greater than that of the joint in a joining process.

1.2.4 Multiple Finishing Techniques

Die cast parts can be produced with smooth or textured surfaces and they are easily plated or finished with a minimum of surface preparation.

1.2.5 Simplified Assembly

Die casting provides integrated fastening elements such as bosses and studs. Holes can be cored and made to tap drill size or external threads can be cast. (www.webcitaion.org).

1.3 ALUMINUM A380 AND A1350 ALLOYS

Certain general importance related to the use of aluminum A1350, as distinct from other aluminum alloys, is their application as electrical conductors which principally are:

1.3.1 ***Conductivity****:* More than twice that of copper

1.3.2 ***Light weight****:* Ease of handling, low installation costs, longer spans, and more distance between pull-ins.

1.3.3 Strength: A range of strengths from dead soft to that of mild steel, depending on the electrical conductor.

1.3.4 Workability: Permitting a wide range of processing from wire drawing to extrusion or rolling and excellent bend quality.

1.3.5 Corrosion resistance: A tough, protective oxide coating quickly forms on freshly exposed aluminum A1350 and it does not thicken significantly from continued exposure to air. The inherent corrosion resistance of aluminum A1350 is due to the thin, tough oxide coating that forms directly after a fresh surface is exposed to air and is well suited for ocean shore applications as well as for usual industrial and chemical atmospheres.

1.3.6 Creep: Like all metals under sustained stress, there is a gradual deformation over a term of years but the extent of creep is determined by the properties of the metal involved, applied stress, temperature and time under load. For example, hard-drawn 1350-H19 aluminum wire in stranded cables under a steadily applied load of about 70 percent of its minimum yield strength will creep approximately 0.4 to 0.6 percent of initial length in 10 years.

1.3.7 Compatibility with insulation: Does not adhere to or combine with usual insulating materials. No tin-coating required and clean stripping.

Also typically using an aluminum A380 casting to replace an iron casting will result in cutting the component and overall weight by half which means that automobile manufacturers are investigating potential applications in areas including engine, drive train and suspension components which made most applications make use of the A 300 series, aluminum - silicon series alloys, particularly the hypoeutectic alloys.

The silicon gives good fluidity when casting, enabling thin sections to be successfully cast. The magnesium provides strength (through heat treatment) while maintaining reasonable ductility. Also the lowest cost general purpose alloy is A380 and is frequently used in the aerospace industry and the ductility is better than that of many wrought alloys. The cast alloys incorporating copper generally have the highest strengths at elevated temperatures. An important feature of aluminum and its alloys (and other non - ferrous alloys) is that unlike ferrous alloys that exhibit finite fatigue endurance strength, the fatigue strength of aluminum alloys continues to fall with increasing stress cycles and this must be accounted for in the design process. Experience may however permit the requirements to be more accurately defined. Porosity of cast components can have a significantly deleterious effect on the fatigue strength of aluminum castings and care must be taken to minimize the entrapment of gas during casting hence a need to evolve other procedures that can limit or minimize this defect in the die casting process. (www.tech/info/al-alloys/imptce.com). uploaded dec- 6- 2012

1.4 STATEMENT OF PROBLEM

Die casting is utilized to produce many products in the current global market. Unfortunately, conventional die casting has a major limitation that is preventing its use on a broader scale. A potential defect, commonly found in die cast components, is porosity.

Porosity often limits the use of the conventional die casting process in favor of products fabricated by other means because it results in leakages of fluids.

Leakages tend to occur in die cast products like pumps, valves, gaskets, e.t.c over some time, compromising the integrity of the product.

Durability of die cast products is reduced as porosity affects the mechanical properties of die cast components. In structural applications, porosity can act as a stress concentrator creating initiation sites for cracks.

1.5 PRESENT RESEARCH

Although much work has been done on various casting processes including die casting, especially on regulation of certain variables like speed, pressure, temperature e.t.c, no work has been reported in the literature which explains effects of pressure on the microstructure and mechanical properties of die cast aluminum alloys A380 and A1350. Moreover, no work has been reported in the literature which optimizes a cold chamber die casting process parameter using A380 and A1350 aluminum alloy. These alloys have a very wide number of applications in aeronautic, automotive, electrical industries and domestic use but still not much work has been done on their properties with different input process parameters.

1.6 RESEARCH JUSTIFICATION

The effects of casting pressure on the properties of aluminum die castings would hopefully reduce porosity and improve the microstructure and mechanical properties. These improved properties of products should meet the requirements needed for many applications. Furthermore industries could easily relate the parameters used and further improve on their product qualities and standards.

The results of this research can be applied to practical foundry problems for manufacturing castings of better properties, and also contribute in many ways to further improving the quality standards for aluminum die casting by:

1. Provision of good quality and durable castings by reduction of defects such as porosity and shrinkage.

2. Provisions of a cleaner atmosphere since most aluminum die casting processes are environmentally friendly.

3. Enhance more usage of die castings.

4. Increase optimization in die casting production lines.

5. Ensure that castings are less prone to rejection and functions maximally in its operation.

1.7 AIM AND OBJECTIVES

The aim of this research is to study the effects of pressure on the microstructure and mechanical properties of aluminum die castings which will be of better qualities and free from defects. The specific objectives are to:

1. Evaluate the influence of different applied pressures on the mechanical properties and microstructures of die cast aluminum A380 and A1350.

2. Compare the mechanical properties of both alloys.

3. Study the grain size and numbers of both alloys.

4. Establish the level of porosity in both alloys.

CHAPTER TWO

LITERATURE REVIEW

2.1 INTRODUCTION

Die casting is a manufacturing process that can produce geometrically complex metal parts through the use of reusable molds, called dies. The die casting process involves the use of a

furnace, metal, die casting machine, and die. The metal, typically a non-ferrous alloy such as aluminum or zinc, is melted in the furnace and then injected into the dies in the die casting machine. There are two main types of die casting machines mainly hot chamber machines (used for alloys with low melting temperatures, such as zinc) and cold chamber machines (used for alloys with high melting temperatures, such as aluminum). However, in both machines, after the molten metal is injected into the dies, it rapidly cools and solidifies into the final part, called the casting. The castings that are created in this process can vary greatly in size and weight. Metal housings for a variety of appliances and equipment are often die cast. Several automobile components are also manufactured using die casting, including pistons, cylinder heads, and engine blocks. Other common die cast parts include propellers, gears, bushings and valves. (www.webcitaion.org)

In the aluminum die casting process, solid ingots of aluminum are melted in furnaces at approximately 650 – 720 ^{0}C. Once liquefied, the aluminum metal is picked up using a ladle and poured by hand or robotically into a steel shot sleeve. The molten aluminum is then injected with hydraulic pressure into the two halves of the die. The molten aluminum metal is then held under high pressure until the metal solidifies, usually within a matter of 2-15 seconds depending on the size of the parts. The die halves are then opened and the part ejected and removed by hand or robotically (www.webcitaion.org).

2.1.1 Hot Chamber Die Casting Process:

Hot chamber machines are used primarily for zinc, lead and other low melting point alloys that do not readily attack and erode metal pots, cylinders and plungers. The injection mechanism of a hot chamber machine is immersed in the molten metal bath of a metal holding furnace. The furnace is attached to the machine by a metal feed system called a gooseneck. As the injection cylinder plunger rises, a port in the injection cylinder opens,

allowing molten metal to fill the cylinder. As the plunger moves downward it seals the port and forces molten metal through the gooseneck and nozzle into the die cavity. After the metal has solidified in the die cavity, the plunger is withdrawn, the die opens and the casting is ejected.

A complete die casting cycle can vary from one second for small component to three minutes for the casting of lager components. This makes the die casting process the faster technique for producing precise non ferrous metal parts. (www.webcitaion.org).

The schematic arrangement of the process is shown in Figure 2.1.

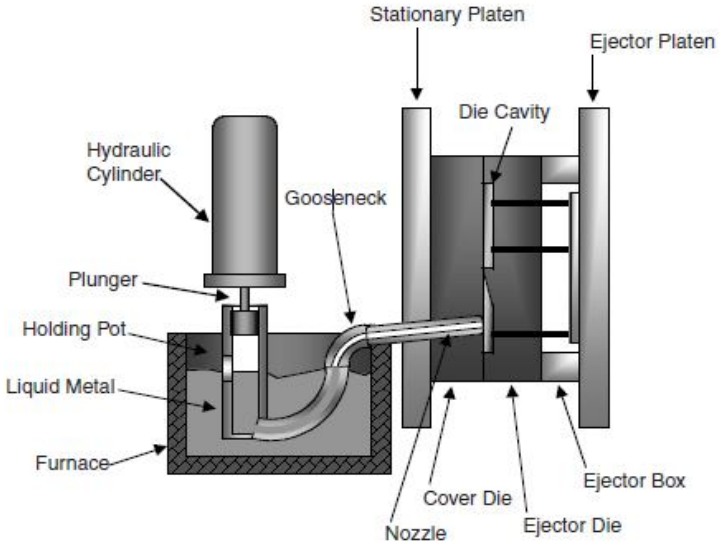


Figure 2.1 Hot Chamber Die Casting Machine (Doehler, 1951)

The Hot-chamber die casting cycle process is as follows:

(a) With die closed and plunger withdrawn, molten metal flows into the chamber.

(b) Plunger forces metal in chamber to flow into the die, maintaining pressure during cooling and solidification.

(c) The plunger is withdrawn, die is opened, and solidified part is ejected.

2.1.2 Cold Chamber Die Casting Process

The cold chamber die casting process is used with higher-melting-point alloys, such as aluminum. Since the cold chamber is located outside of the furnace, as compared to hot chamber, it requires a means of moving the molten metal from the holding furnace to the cold chamber. The cold chamber is attached between the die casting machine front platen and the die. The transport of the molten metal is typically done with a ladle mechanism, either manually or automatically, when casting aluminum alloys. Casting cycle times can range from 10 s for a small machine to 2 min for a large machine (ASM handbook (2008)). In the cold chamber process, the molten metal is ladled into the cold chamber for each shot, as shown in Figure 2.2, There is less time exposure of the melt to the plunger walls or the plunger. This is particularly useful for metals such as aluminum, copper and its alloys**.** Die casting molds tend to be expensive as they are made from hardened steel and also the cycle time for building these is long. The stronger and harder metals such as iron and steel cannot be die cast.

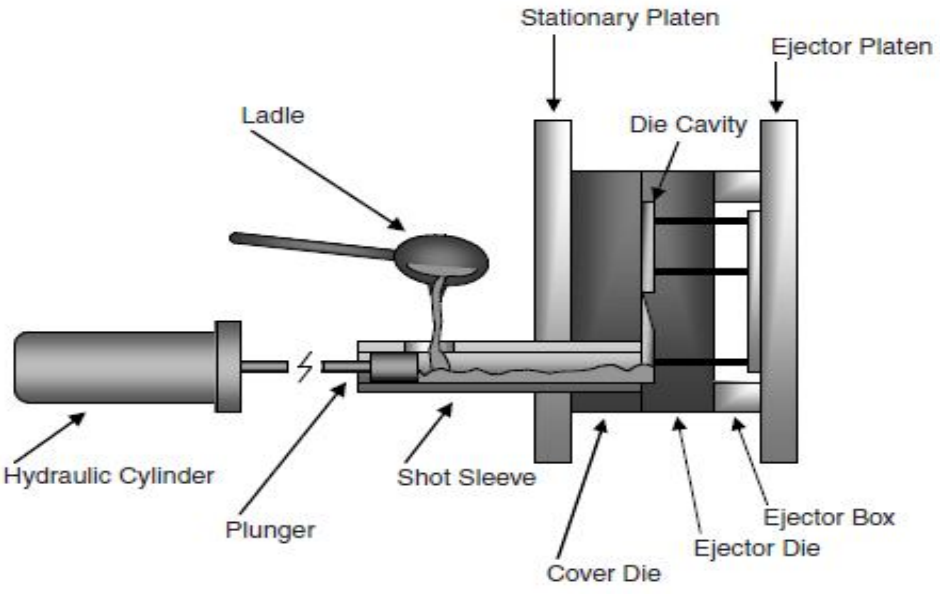


Figure 2.2 : Cold Chamber Die Casting Machine (Doehler, 1951)

The Cold-chamber die casting process cycle is as follows:

(a) With die closed and plunger withdrawn, molten metal is poured into the chamber;

(b) The plunger forces metal to flow into the die, maintaining pressure during the cooling and the solidification; and

(c) The plunger is withdrawn, the die is opened, and the part is ejected. It is used for higher melting temperature metals e.g. aluminum, copper and their alloys.

Discontinuities are a common problem in die castings. Discontinuities are irregularities, breaks, or gaps in the material structure. Some types of casting discontinuities are visible to the naked eye and are caused by variation in the casting process. However, most of them are not detectable by visual inspection because they occur below the surface of the material. The sub-surface is the most highly loaded region of the material. Therefore, sub-surface discontinuities such as porosity greatly influence the ability of a component to withstand load (Duckett, 1988).

The aluminium die casting industry is one of the foremost suppliers of castings to the automotive industry. The role of the die casting manufacturer is to deliver high quality castings to this industry. The manufacturer is usually required to replace the castings if found defective during the customer's machining process. This places a financial burden on the manufacturer. The avoidance of discontinuities prior to the transfer of products to the client not only saves money and time, but also enhances the manufacturer's reputation in relation to quality. Therefore, it is essential to evolve ways that will assist the die casting industry to achieve quality assurance and to remain competitive in the international market (Rickards et al, 1994).

With the emergence of modern design techniques and aluminium alloys, the mechanical strength of die castings is usually of concern because automotive die castings are often in

contact with fluids under pressure, including transmission fluid, engine oil and coolant. Hence, a more likely problem is that, the castings with defects are subjected to leakage under pressure. Therefore, die casting manufacturers must make sure defects are avoided that may cause leakage under pressure prior to supplying them to their customers. These defects primarily relate to porosity and cracks.

In the 21st century, die casting manufacturers need to maintain standards and keep abreast of the latest technologies to be competitive in the international market.

George Johnson expressed a similar view in his keynote address on "The People / Technology Partnership". *"To survive and prosper in the coming years, successful foundries will have to be leaders in quality, cost, technology and response to customer needs"* (Duckett, 1988). Even though this statement was made in the early 1990's, it remains valid for casting industries.

Though tremendous technological advancements in the metal casting industry have taken place in recent years, the foundry industry faces increasing demands to achieve higher productivity at minimum cost, even while producing high quality cast components of intricate shapes. By proper selection of a casting technique with careful foundry and metallurgical controls, castings of high quality can be commercially manufactured. Under the present scenario of industrial development, metal casting has moved from an art and craft industry to the industry based on science and technology. The pressure die casting manufacturing processes have been systematically developed so that structure may be controlled and quality may be assured. Die casting provides the foundry man with one of the fastest means of producing castings with a much higher degree of accuracy than that normally obtained by conventional sand casting.

Pressure die casting of aluminum alloys offers means for very rapid production of engineering and other related components of even or intricate design. The technique has

obvious advantages when a component is required in large quantities. However, for engineering components such as those required for aeronautic, space, defense and automotive applications, mechanical properties and durability are of primary importance. It is therefore essential that the best features of design should be employed and optimum casting techniques with minimum costs be adopted. Essentially, die casting uses steel molds called dies into which molten metal is forced using extremely high pressure. Die casting is a versatile technique that allows for various levels of complexity in production, while still maintaining absolute precision to create a flawless end product (www.tech/info/die-cast.com).

2.2 MATHEMATICAL MODELLING

A model is a description of a system, theory, or phenomenon that accounts for its known or inferred properties and may be used for further study of its characteristics. By these simplifications, good models allow us to obtain an easily understandable, mathematically calculable image of the real world. If a model is formulated with the aid of mathematical relations, we speak of mathematical models (Rutherford et al, 1994).

By extension, a mathematical model is a mathematical structure that can be used to describe and study a real situation. Models are used to express the characteristics of reality which are considered important and to neglect those which seem secondary. Since prehistorical times, simple models such as maps and pre-designed diagrams have been used. A mathematical model usually describes a system by a set of variables and a set of equations that establish relationships between the variables. Variables may be of many types; real or integer numbers,

values or strings, for example. The variables represent some properties of the system, for example, measured system outputs often in the form of signals, timing data, counters, and event occurrence (yes/no). The actual model is the set of functions that describe the relations between the different variables (Korotayev et al 2006).

A mathematical model is a description of a system using mathematical concepts and language. The process of developing a mathematical model is termed mathematical modeling. Mathematical models are used not only in the natural sciences (such as physics, biology, earth science, meteorology) and engineering disciplines (e.g. computer science, artificial intelligence), but also in the social sciences (such as economics, psychology, sociology and political science); physicists, engineers, statisticians, operations research analysts and economists use mathematical models most extensively to help explain a system and to study the effects of different components, and to make predictions about their behavior on the system. Mathematical modeling is the process of using various mathematical structures - graphs, equations, diagrams, scatter plots, tree diagrams, and so forth - to represent real world situations. The model provides an abstraction that reduces a problem to its essential characteristics. Mathematical models can take many forms, including but not limited to dynamical systems, statistical models, differential equations, or game theoretic models (Alaxander et al, 2002).

Mathematical models are useful for a variety of reasons. Foremost, models represent the mathematical core of a situation without extraneous information. The equation a = b + 6, for instance, removes all of the unnecessary words from the original statement "Alison is 6 years older than Brenda." In addition, people can use models to explore various scenarios cost-effectively. A jet engine manufacturer would prefer to design a mathematical model and conduct simulations on a computer, rather than incur the costs of building engines for testing

purposes and also when engineers analyze a system to be controlled or optimized, they use a mathematical model. In analysis, engineers can build a descriptive model of the system as a hypothesis of how the system could work, or try to estimate how an unforeseeable event could affect the system. Similarly, in control of a system, engineers can try out different control approaches in simulations (Cha et al, 2000).

In general, mathematical models may include logical models, as far as logic is taken as a part of mathematics. In many cases, the quality of a scientific field depends on how well the mathematical models developed on the theoretical side agree with results of repeatable experiments. Lack of agreement between theoretical mathematical models and experimental measurements often leads to important advances as better theories are developed.

2.3 REVIEW OF PAST WORK

Adler *et al (1989)* investigated porosity defects in aluminium cast materials, and used volumetric analysis to identify gas porosity defects. They studied the effect of backscatter in their work on the ultrasonic inspection of aluminium cast materials.

Ambardar *et al (*1996) investigated the effects of surface roughness and grain structure variations on ultrasonic signals obtained from sample aluminium die casting blocks using the backscattering of ultrasonic sound method. In these investigations, the arithmetic mean surface roughness (Ra) values were in the region of 50 μm. The results of their investigation led to the conclusion that an increase in surface roughness decreased the back wall echo component of the ultrasonic signal.

Aweda, (2006) investigated on temperature distribution and properties in squeeze casting of aluminum and concluded that applied pressure and die temperatures are found to have significant effects on the heat transfer coefficients of aluminum. Heat transfer coefficients decrease sharply when the casting temperature of the metal is near liquidus. Therefore the effect of pressure application on the solidifying aluminum is more pronounced within the first 40 seconds of pouring molten aluminum metal into the mould cavity.

Chiang et al (2008) proposed mathematical models for the modeling and analysis of the effects of machining parameters on the performance characteristics in the high pressure die casting (HPDC) process of Al–SI alloys which were developed using the response surface methodology (RSM) to explain the influences of three processing parameters (die temperature, injection pressure and cooling time) on the performance characteristics of the mean particle size (MPS) of primary silicon and material hardness (HBN) value and found that two main significant factors involved in the mean particle size of primary silicon were the die temperature and the cooling time and that the injection pressure and die temperature also have statistically significant effect on microstructure and hardness.

Dahle *et al* (2002) investigated the effects of pressure on density and porosity in an aluminum cast by applying pressure to the riser in a permanent mold (die) and found that a flat distribution, this time of density rather than porosity was observed with the pressurized riser.

Dargusch et al (2006) determined the effects of process variables on the quality of high pressure die cast components with the aid of in-cavity pressure sensors. In particular, the effects of set intensification pressure, delay time, and casting velocity were investigated and

in turn the effect of variations in these parameters on the integrity of the final part. Porosity was found to decrease with increasing intensification pressure and increase with increasing casting velocity.

Li et al (2003) investigated the effect of pressure on microstructure and mechanical properties of Al-Cu-based alloy prepared by squeeze casting and concluded that hardness, tensile strength and ductility of ZA27 squeezed castings are greatly affected by applied pressure. Also the results of DTA and SEM show that at high specific pressure, the eutectic reaction of squeeze cast ZA27 alloy is restrained, and the final solidified structure is (η+ε) phases instead of eutectic phase (β+η+ε) *and* the primary reaction is promoted in squeeze cast ZA27 alloy solidified at high pressure and the fine microstructure is obtained with the increase in pressure.

Sabau and Viswanathan (2002) developed a comprehensive methodology that takes into account solidification, shrinkage-driven inter-dendritic fluid flow, hydrogen precipitation, and porosity evolution for the prediction of the micro porosity fraction and distribution in aluminum alloy castings. The approach may be used to determine the extent of gas and shrinkage porosity, *i.e.*, the resultant micro porosity which occurs due to gas precipitation and that which occurs when solidification shrinkage cannot be compensated for by the inter-dendritic fluid flow. The results showed that the effect of micro porosity on the inter-dendritic fluid flow cannot be neglected.

Suresh, **(2006)** investigated die-cast sub surface flaws and defects by an ultrasonic inspection of gas porosity defects in aluminium die-castings.

Watmough, (1960) suggested a radically different series of experiments, whereby end-fed two-inch and four-inch square sectioned sand-cast bars were poured into three aluminum base alloys and plaster sleeved risers pressurized. The work compared the effects of 0, 10, 20 psi (0, 0.069, and 0.138MPa) pressure levels on the X-ray soundness of vertical slices taken along lengths of the bars concerned, In addition to the above examination of casting slices, sectioning of the risers of the 5% silicon alloy bars revealed an interesting effect, the contrast between the non-pressurized and the pressurized risers was striking; that associated with the pressurization piped in the fashion of a short freezing range alloy, the non-pressurized riser did not as would be expected.

Ying-hui et al (2009) investigated microstructures and properties of die casting components with various thicknesses made of AZ91D alloy by means of a scanning electron microscope (SEM), transmission electron microscope (TEM), high-resolution transmission electron microscope (HRTEM), etc. It was concluded that mechanical properties of the die casting components mainly depend on grain size of -Mg phase.

Yoshihiko and Soichiro (2009) identified the cause of porosity and took corrective action in the die-casting process accurately and rapidly, a quantitative estimation of the morphology of pores can be an effective technique. In this study, fractal analysis was used to characterize porosity quantitatively in terms of the spatial distribution of a number of pores appearing in a target region. The purpose of the investigation was to evaluate the proposed fractal analysis by comparing the porosity in two types of aluminum alloy die castings manufactured by different die-casting processes, and to confirm that fractal analysis of the spatial distribution of pores can quantitatively characterize the porosity.

Zhu et al (2006) developed a numerical model for predicting micro porosity formation in aluminum castings, which describes the redistribution of hydrogen between solid and liquid phases, the transport of hydrogen in liquid by diffusion, and Darcy flow in the mushy zone. One of the key features of the model is that it uses a two-stage approach for porosity prediction. In the first stage, the volume fraction of porosity is calculated based on the reduced pressure, whereas, in the second stage, at fractions solid greater than the liquid encapsulation point, the fraction porosity is calculated based on the volume of liquid trapped within the continuous solid network, which is estimated using a correlation based on the Niyama parameter. The porosity model was used in conjunction with a thermal model solved using the commercial finite-element package ABAQUS. The parameters influencing the formation of micro porosity were discussed including a means to describe the super saturation of hydrogen necessary for pore nucleation. The model has been applied to examine the evolution of porosity in a series of experimental samples cast using unmodified A356 in which the initial hydrogen content was varied from 0.048 to 0.137 (cc/100 g). A comparison between the model predictions and the experimental measurements indicated good agreement in terms of the variation in porosity with distance from the chill and the variation resulting from initial hydrogen content.

Kumar (2010) developed a multi- response optimization model of process parameters in die cast aluminum LM6 alloy by evaluating temperature of the molten metal, injection pressure of the molten metal, type of coating and type of cooling on the density, hardness and surface roughness of aluminum LM6 alloy. An experimental model for encompassing three responses namely surface roughness, density and hardness was employed to carry out the experiment and an analysis of variance (ANOVA) was performed for all the responses and

the effect of the factors were explained and regression analysis was done to correlate the effect of factors with all the three responses.

The result of ANOVA showed that the main significant factor in multi response signal (MRSN) calculation was the injection pressure and the MRSN is maximized with increase in temperature and the cooling time and that the MRSN is not affected by coating and that water cooling increased the hardness as compared to air and oil cooling. He further concluded that higher injection pressures were more suitable in casting of aluminum alloys, also the analysis of microstructure showed structured changes observed in all samples and that porosity present in a casting generally decreases as the pressure in the die casting increases.

CHAPTER 3

MATERIALS AND METHODS

3.1 MATERIALS

The materials shown in figures 3.1 and 3.2 that were used in this work are aluminum alloys A380 (used mostly in aeronautics) and A1350 (used mostly for electric distribution lines) these were procured, cut and melted in an electric furnace of capacity of 500kg available at the Scientific and Equipment Development Institute (SEDI), Enugu.



Figure 3.1: Material of A1350 before casting



Figure 3.2: Material of A380 before casting

3.1.1 Chemical composition of work piece materials

X- Ray Florescent test

X-ray fluorescence (XRF) is the emission of characteristic "secondary" (or fluorescent) X-rays from a material that has been excited by bombarding with high-energy X-rays or gamma rays. The phenomenon is widely used for elemental analysis and chemical analysis, particularly in the investigation of metals, glass, ceramics and building materials, and for research in geochemistry, forensic science and archaeology. The use of a primary X-ray beam to excite fluorescent radiation from a metal sample was first proposed by Glocker and

Schreiber in 1928. Today, the method is used as a non-destructive analytical technique, and as a process control tool in many extractive and processing industries.

When materials are exposed to short-wavelength X-rays or to gamma rays, ionization of their component atoms may take place. Ionization consists of the ejection of one or more electrons from the atom, and may occur if the atom is exposed to radiation with energy greater than its ionization potential. X-rays and gamma rays can be energetic enough to expel tightly held electrons from the inner orbitals of the atom. The removal of an electron in this way renders the electronic structure of the atom unstable, and electrons in higher orbitals "fall" into the lower orbital to fill the hole left behind. In falling, energy is released in the form of a photon, the energy of which is equal to the energy difference of the two orbitals involved. Thus, the material emits radiation, which has energy characteristic of the atoms present. The term fluorescence is applied to phenomena in which the absorption of radiation of a specific energy results in the re-emission of radiation of a different energy (generally lower) (Beckhoff et al, 2006).

X-ray is a type of electromagnetic wave such as visible light ray, but the key difference is its extremely short wavelength, measuring from 100A to 0.1A. And compared to normal electromagnetic waves, X-ray easily passes through a material and it becomes stronger as the material's atomic number decreases. X-ray fluorescence analysis is a method that uses the characteristic X-ray (fluorescent X-ray) that is generated when X-ray is irradiated on a material. The fluorescent X-ray is the excess energy irradiated as electromagnetic field, which is generated when the irradiated X-ray forces the constituent atom's inner-shell electrons to the outer shell and the vacant space (acceptor) falls on the outer-shell electrons. The generation of fluorescent X-ray is shown in Figure 3.3

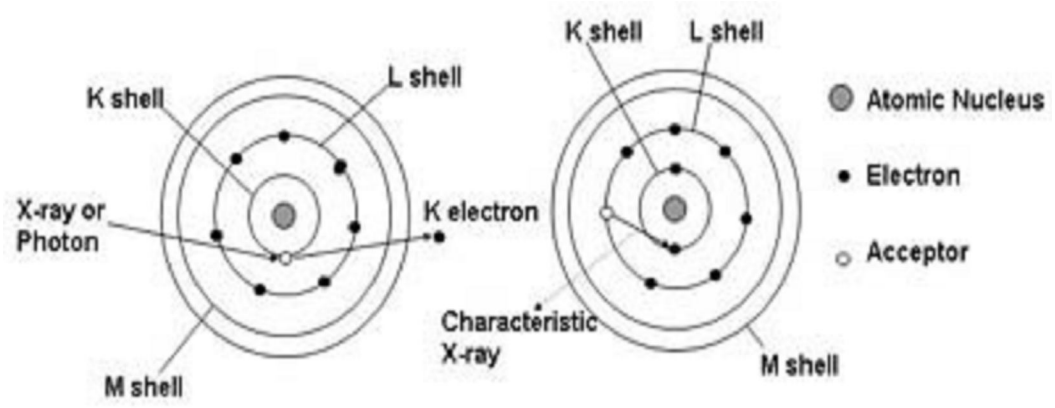


Figure 3.3: X-ray generation schematics (Jenkins et al, 1973).

Since X-ray fluorescence analysis can analyze a sample non-destructively and quickly, it can be applied to a wide range of uses such as manufacturing and quality control. Recently, as techniques for high-sensitivity, technologies such as filtering and lamination have been applied to eliminate the interference of background, which made measurement of trace amounts possible (Jenkins et al, 1973).

The XRF test was carried out using the XRF machine at the physics laboratory of the Science and Technology Complex (SHEDA) Abuja. Chemical composition of both alloys as revealed by the x-ray fluorescence test is summarized in the Table 3.1

Table 3.1: Chemical composition of work piece materials

	percentage composition								
	Al	**Si**	**Cu**	**Mg**	**Mn**	**Zn**	**Ni**	**Ti**	**Fe**
A380	**Bal**	**8.50**	**3.50**	**0.05**	**0.27**	**1.80**	**0.08**	**0.05**	**1.05**
	percentage composition								

	Al	Si	Fe	Cu	Mn	Cr	Zn	others
A1350	**Bal**	**0.10**	**0.40**	**0.05**	**0.01**	**0.01**	**0.05**	**0.15**

3.2 EQUIPMENT

The main items of equipment for this work were:

(1) Horizontal cold chamber pressure die machine

(2) Electrical furnace for melting aluminum

(3) Optical and scanning electron microscopes

(4) Measuring instruments and gauges

(5) Rockwell hardness testing machine

3.2.1 EXPERIMENTAL PROCEDURE

The different casting procedures are described thus: Five die casting samples of each alloy were produced under different pressure ranges as done by Kumar, (2010).

The machine was operated at standard operating conditions except the injection pressure which was varied at 0, 350, 700, 1050 and 1400 kg/cm^2 as per experimental design. The metal was poured into the injection chamber in the injection sleeve with the aid of a pouring spoon. The experiments were conducted in the foundry section of the central

workshop at the Scientific and Equipment Development Institute (SEDI) Enugu. An electric furnace was used for melting the A380 and A1350 alloys and the pressure in the die casting machine was controlled by the pressure regulating valve on the machine.

3.3 METHODOLOGY

3.3.1 POURING AND MELTING

Aluminum alloys A1350 and A380 were procured and melted in an electric furnace of capacity 500kg at the Scientific and Equipment Development Institute, Enugu. (SEDI), at a temperature of 720^{o}C. The dies were prepared by spraying the mold cavity with a lubricant. The lubricant helped to control the temperature of the die and also assist in the removal of the casting. The die was then closed and molten metal injected into it at various pressure levels. Once the mold cavity was filled, the pressure was applied until the casting solidified. The die was then opened and the solid casting removed. The whole process was done for both alloys to compare and confirm results.

3.3.2 PRESSURE APPLICATION

The injection pressure was regulated to permit five pressure levels by a pressure regulating valve on the die casting machine and each phase of the experiment was described separately. The specimen of both alloys were die cast separately and the effects of the five pressure levels on the mechanical properties and microstructure of the specimen of both alloys were investigated. The machine was operated at standard operating conditions except the injection pressure which was varied at 0, 350, 700, 1050, and 1400kg/cm^2 for the experiment to allow for comparison for both alloys.

3.4 DESCRIPTION AND SPECIFICATION OF DIE CASTING MACHINE

The experiments were conducted on a horizontal cold chamber pressure die casting machine at the Scientific and Equipment Development Institute (SEDI), Enugu, specifications of which are given in table 3.2

Table 3.2 Specifications of Die Casting Machine

SPECIFICATIONS	METRIC
Locking force	500 tons
Injection force	49 tons
Ejection force	24 tons
Stationary platen (W x H)	1070 ×1070 (mm)
Movable platen (W x H)	1070 × 1070 (mm)
Max. die height	800 mm
Tie bar diameter	140 mm
Die stroke	560 mm
plunger stroke	580 mm
Ejection stroke	110 mm
Shot tip penetration	250 mm
Electric motor capacity	34.5 kw
Low shot speed	600 mm/s
Hydraulic pump (vane type)	400 ltr/min
Machine size (L X W X H)	7.4 x 2.1 x 2.5 m
Machine weight	26.3 tons
High Shot speed	4500 mm/s

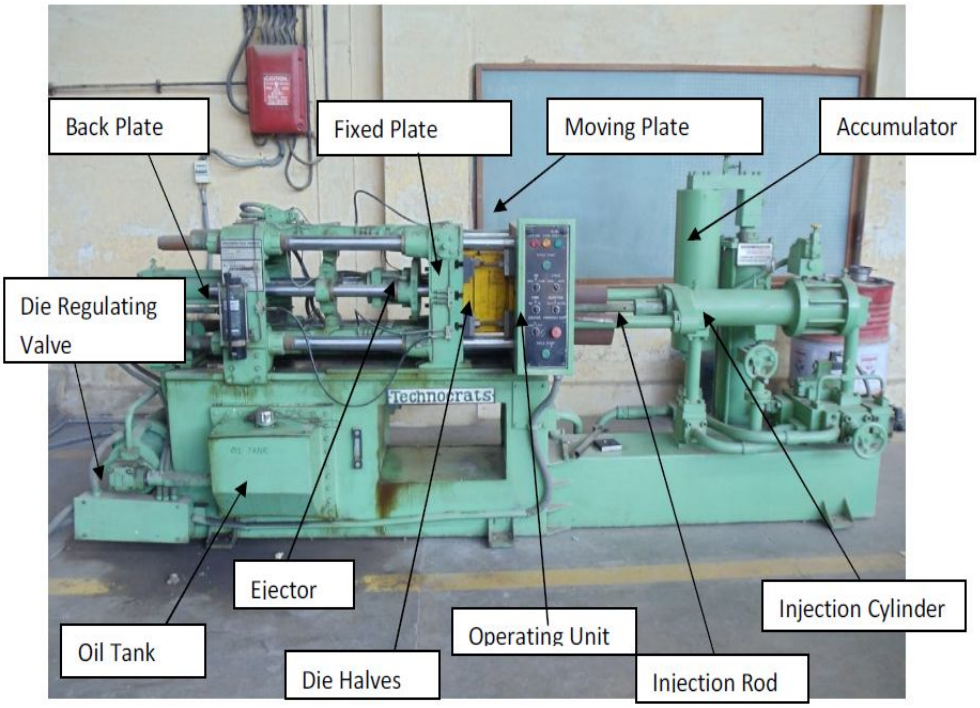


Figure 3.4 High Pressure Cold Chamber Die Casting Machine at (SEDI Enugu).

The main parts of the machine shown in figure 3.3 are the control box panel, fixed plate, moving plate, back plate, accumulator, injection cylinder, injection rod, ejector system, oil tank, dies regulating valve, pressure regulating valve. The injection pressure can be varied through the pressure regulating valve. Control is provided on the machine for die opening time, closing time and the ejector time for the ejection of cast product. The machine can be operated in manual as well as in automatic modes.

3.4.1 Operating mode

(a) Manual Mode: In this mode the machine is not under the casting program. Direction of operations depends upon the decision of the operator.

(b) Automatic Mode: Machine operations can be programmed e.g. die opening time, die closing time; casting ejection time can be controlled.

(c) Stop Button: The machine stops when the stop button is pushed.

3.4.2 Display indication

Pressure gauge: the pressure gauges are used to display the pressure of injection of molten metal and to display the pressure of the accumulator.

3.5 DIES FOR EXPERIMENT

Since dies are very expensive to construct and build, dies used for the casting of top cylinders of a vulcanizing machine available at the Scientific and Equipment Development Institute (SEDI), Enugu were used to cast the samples of both alloys and specimen were cut from them for mechanical tests and microstructure analysis. Dies used for the casting of the samples were made of alloyed steel in two sections, one was the fixed die half and the other was the ejector die half to permit the removal of casting. A sprue hole was in the fixed die that allowed the molten metal enter the die and fill the cavity. The temperature in the die, measured with thermocouples, was in the range of 200 to 300^{o}C. The die had locking pins to secure the two halves and ejector pins to help remove the cast part.

3.5.1 Samples after Casting

The final cast samples of both alloys that were regulated under different applied pressures in the casting process are shown below in figures 3.5 and 3.6 and are represented in the table 3.3:



Figure 3.5: Samples of A1350 after casting



Figure 3.6: Samples of A380 after casting

Table 3.3 Input factors and their respective levels of samples shown above

Sample No (A380)	Sample No (A1350)	Pouring temp ^{0}C	Injection pressure (Kg/cm$^{2)}$	Coating type	Cooling medium
1	1	720	1400	graphite oil	Water + oil
2	2	720	1050	graphite oil	Water + oil
3	3	720	700	graphite oil	Water + oil
4	4	720	350	graphite oil	Water + oil
5	5	720	0	graphite oil	Water + oil

3.6 MECHANICAL TEST PROCEDURE

3.6.1 Tensile Test

The tensile test is a fundamental test in which a sample is subjected to uniaxial tension until failure and also indicates the ability of a metal to withstand forces that stretch the material prior to failure. The tensile test process involved machining the cast samples to tensile specimen and placing the test specimen in the testing machine and applying tension to it until it fractures. During the application of tension, the elongation of the gauge section was recorded against the applied force. The specimen were subjected to tensile tests in accordance with the ASTM E8 standard test method for tension testing of metallic materials using a Hounsfield tensiometer with maximum load of 500KN available at the workshop of the Science and Technology Complex (SHEDA) Abuja. The test specimen size was 100.4mm length and gauge length of 45mm was marked on the samples. The specimen were mounted by their ends into the holding grips of the testing machine and locked securely. The machine

then elongated the specimen at constant rate and at the same time the instantaneous load applied was measured using an extensometer and recorded. (ASTM, 2008).

3.6.2 Hardness Test

The hardness values of the samples were measured using the Rockwell hardness testing machine (model AVERY 6402 England), available at the workshop of the Science and Technology Complex (SHEDA) Abuja. The indents formed were measured on B scale with a minor load of 10 kg, major load of 100kg but before the hardness test, the surfaces of the samples were cleaned thoroughly by removing dirt, scratches and oil.

Each sample of both alloys was placed on the anvil that supports the test samples and a minor load of 10kg was applied to the samples in a controlled manner without vibration and a zero datum position was established and then a major load of 100kg was applied and reading was taken as the pointer comes to rest for 20 seconds and the load was removed and the hardness value read from the digital scale. (ASTM, 2008)

3.6.3 Impact Test

The impact tests of the samples were conducted using the Avery Denison test machine available at the workshop of the Science and Technology Complex (SHEDA) Abuja. Impact tests of the samples of both alloys were carried out using the charpy V notch test method. All specimen were notched at the centre to about 2mm depth with a root radius of 0.25 mm at angle of 45^0 according to the standard of the machine used. Impact tests conducted for each sample were in accordance with ASTM E23 "standard method for notched bar impact testing of metallic materials". The expended energy was measured and recorded for each specimen. This was used to measure their toughness. (ASTM, 2008)

3.7 MICROSTRUCTURE ANALYSIS

3.7.1. ETCHING AND MICROSCOPY

Metallographies of both alloy samples were investigated by means of a metallurgical microscope available at the metallurgy laboratory at the Federal University of Technology Minna**.**

Preparation of the samples of both alloys for micro examination involved mainly sampling, polishing and etching. Samples measuring 26mm x15mm x 5mm were cut from the castings with the help of a hacksaw. The samples were filed and ground. Grinding was done in succession on a bench grinder using silicon carbide abrasive papers of 220- , 320-, 400-, and 600- grits

The specimen were polished using wet method with final polishing being carried out by hand, and then they were etched in aqueous solution containing 2.5%HNO_3, 1.5 % HCL and 1% HF acid (Keller's reagent) for 20 to 60 seconds. Etching was done to make visible the grains of the samples under different pressure conditions.

3.7.2 Scanning Electron Microscope Analysis

Microstructures of both alloy samples were investigated by means of a scanning electron microscope (SEM) available at the physics laboratory at the Science and Technology Complex (SHEDA) Abuja. Samples were placed on the sample holder with the help of double sided conductive aluminum tape and mounted unto the sample chamber and an electron gun switched on which passed an accelerating voltage of 20kV and probe current of 227pA through the samples at a working distance of 6.0mm. SEM was done to make visible porosity pores across the microstructures of the samples under the different pressure conditions.

3.8 REGRESSION MODELS

Regression models are used to predict one variable from one or more other variables. Regression models provide the scientist with a powerful tool, allowing predictions about past, present, or future events to be made with information about past or present events. The scientist employs these models either because it is less expensive in terms of time or money to collect the information to make the predictions than to collect the information about the event itself, or, more likely, because the event to be predicted will occur in some future time. In order to construct a regression model, both the information which is going to be used to make the prediction and the information which is to be predicted must be obtained from a sample of objects or individuals (Weisberg, 1985). The relationship between the two pieces of information is then modeled with a linear transformation equation. Then in the future, only the first information is necessary, and the regression model is used to transform this information into the predicted. In other words, it is necessary to have information on both variables before the model can be constructed. X is the variable used to predict, and is sometimes called the independent variable, Y is the observed value of the predicted variable, and is sometimes called the dependent variable. The goal in the regression procedure is to create a model where the predicted and observed values of the variable to be predicted are as similar as possible. The more similar these two values, the better the model. Regression analysis is used to establish relationship between two variables (Cook, 1979).

Multiple regression analysis is a statistical tool for understanding the relationship between two or more variables. Multiple regressions involves a variable to be explained called the dependent variable and additional explanatory variables *that* are thought to produce or be associated with changes in the dependent variable for example, a multiple regression analysis

might estimate the effect of the number of years of work on salary. Salary would be the dependent variable to be explained; years of experience would be the explanatory variable. Multiple regression analysis is sometimes well suited to the analysis of data about competing theories in which there are several possible explanations for the relationship among a number of explanatory variables. Multiple regressions typically use a single dependent variable and several explanatory variables to assess the statistical data pertinent to these theories. For example a case alleging sex discrimination in salaries, for example, a multiple regression analysis would examine not only sex, but also other explanatory variables of interest, such as education and experience (Rubinfield et al 1983). Multiple regression also may be useful in determining whether or not a particular effect is present, in measuring the magnitude of a particular effect, and in forecasting what a particular effect would be, but for an intervening event.

Regression residuals *are* the difference between the actual and fitted values of the dependent variable. In general, the residual *e* associated with a data point is given by

$e = Yi - \hat{Y}I$ *where* Yi is the actual values and YI is the predicted or forecasted values which is the error made by the least squares regression method for that individual. *Mean Square Error (MSE).* The estimated variance of the regression error is calculated as the average of the sum of the squares of the regression residuals (allen, 1971).

The linear regression was carried out using the regression line equation $y = a + bx$.

The constants a and b can be calculated from the expressions –

$$a = \frac{(\sum y.\ \sum x^2) - (\sum x.\ \sum xy)}{(N\sum x^2) - (\sum x)^2} \quad \ldots\ldots\ldots\ldots\ldots\ldots\ldots\ldots\ldots\ldots (1)$$

$$b = \frac{N\sum xy - (\sum x\ .\ \sum y)}{(N\sum x^2) - (\sum x)^2} \quad \ldots\ldots\ldots\ldots\ldots\ldots\ldots\ldots\ldots\ldots (2)$$

And the multiple regression was carried out using the multiple regression equation

$y = a + bx_1 + cx_2$ where the equations for the constants are

$$\sum y = na + b\sum x_1 + c\sum x_2 \quad \ldots\ldots\ldots\ldots\ldots\ldots\ldots\ldots\ldots\ldots\ldots\ldots (3)$$

$$\sum x_1 y = a\sum x_1 + b\sum x_1^2 + c\sum x_1 x_2 \quad \ldots\ldots\ldots\ldots\ldots\ldots\ldots\ldots\ldots\ldots\ldots\ldots (4)$$

$$\sum x_2 y = a\sum x_2 + b\sum x_1 x_2 + c\sum x_2^2 \quad \ldots\ldots\ldots\ldots\ldots\ldots\ldots\ldots\ldots\ldots\ldots\ldots (5)$$

3.8.1 Error Analysis

In modeling of real systems, error analysis is concerned with the changes in the output of the model as the parameters to the model vary about a mean. For instance, in a system modeled as a function of two variables (f(x,y) . Error analysis deals with the propagation of the model errors in x and y (around mean values $\bar{x}$ and $\bar{y}$) to error around a mean (James, 1996).

Root mean square error (RMSE)

The Root Mean Square Error (**RMSE**) (also called the root mean square deviation, RMSD) is a frequently used measure of the difference between values predicted by a model and the values actually observed from the environment that is being modeled. These individual differences are also called residuals, and the RMSE serves to aggregate them into a single measure of predictive power.

The RMSE of a model prediction with respect to the estimated variable X_{model} is defined as the square root of the mean squared error:

$$RMSE = \sqrt{\frac{\sum_{i=1}^{n} (X_{obs,i} - X_{model,i})^2}{n}} \quad \text{..... (6)}$$

Where X_{obs} is observed values and X_{model} is modeled values at time/place i.

CHAPTER FOUR

RESULTS AND DISCUSSIONS

4.1 RESULTS

The results of the various tests carried out are shown below in figures 4.1 to 4.14 and tables A1 to A16 in the appendix.

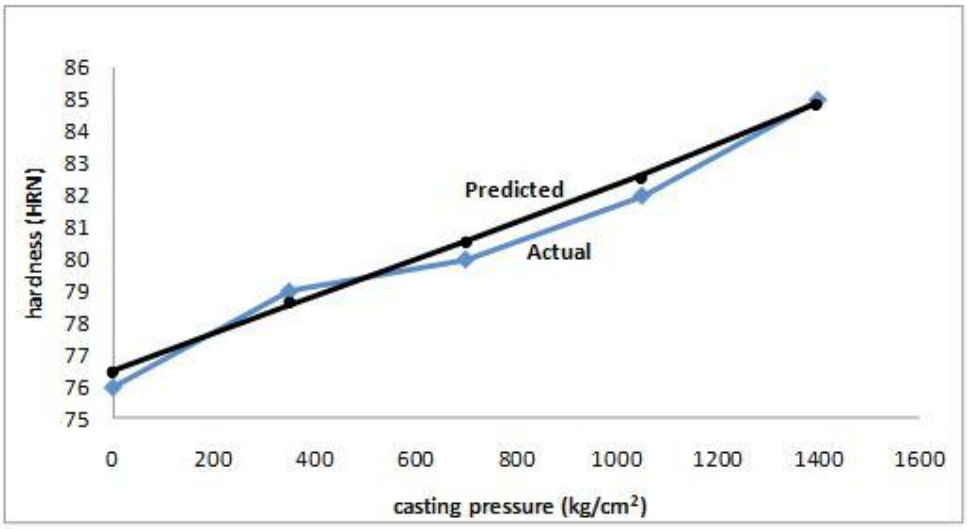


Figure 4.1: Experimental and Predicted Plots of Hardness against pressure of A380

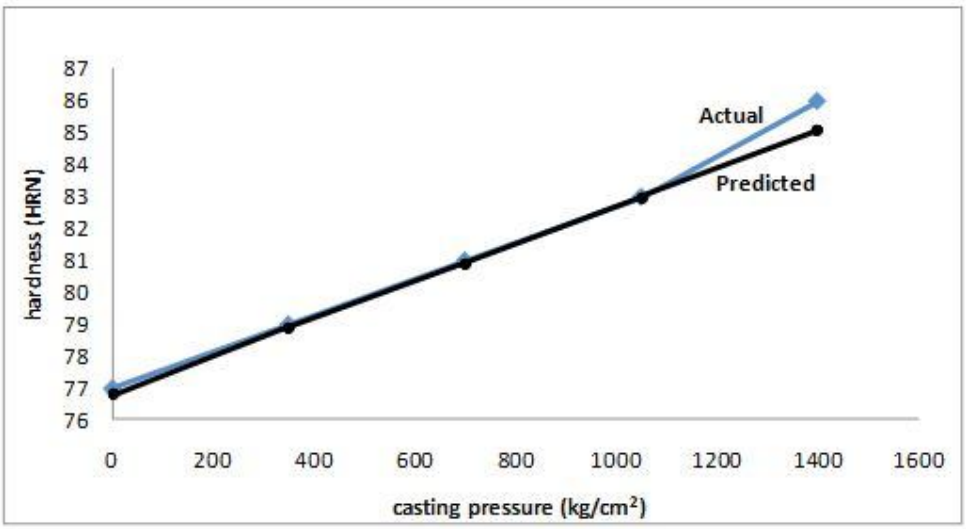


Figure 4.2: Experimental and Predicted Plots of Hardness against pressure of A1350

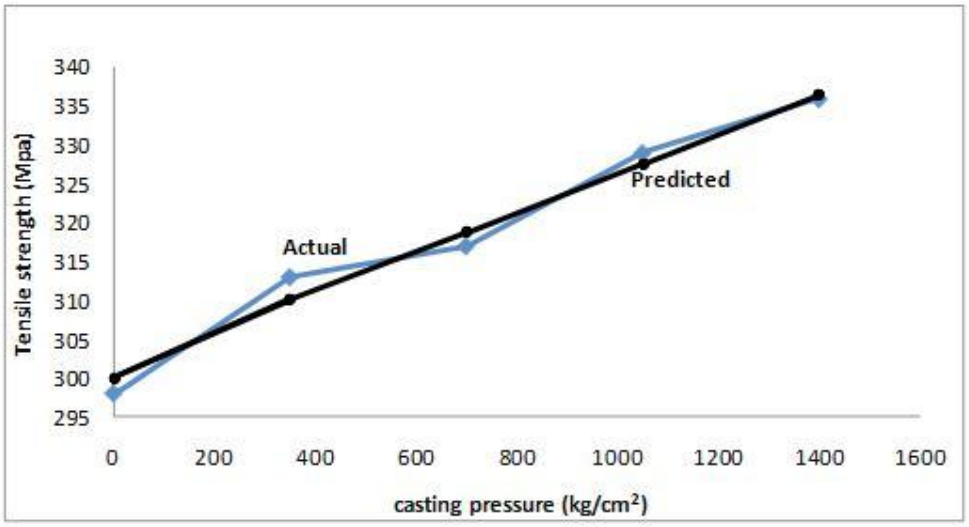


Figure 4.3: Experimental and Predicted Plots of tensile strength vs pressure of A380

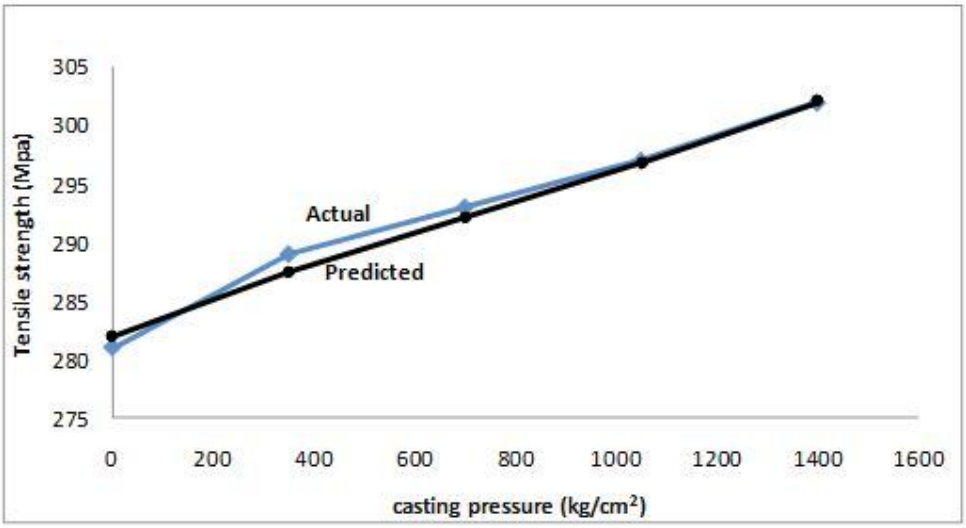


Figure 4.4: Experimental and Predicted Plots of tensile strength vs Pressure of A1350

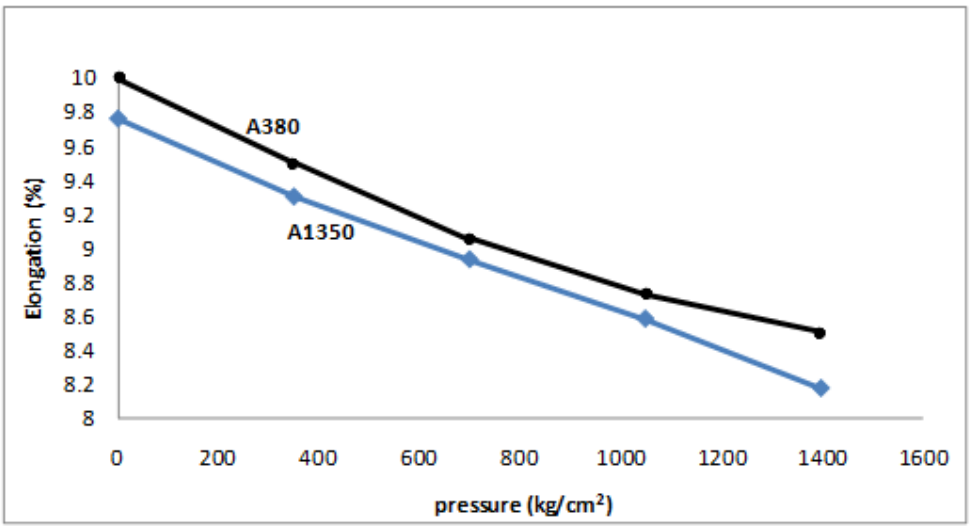


Figure 4.5: Elongation vs Pressure Plots of A380 and A1350

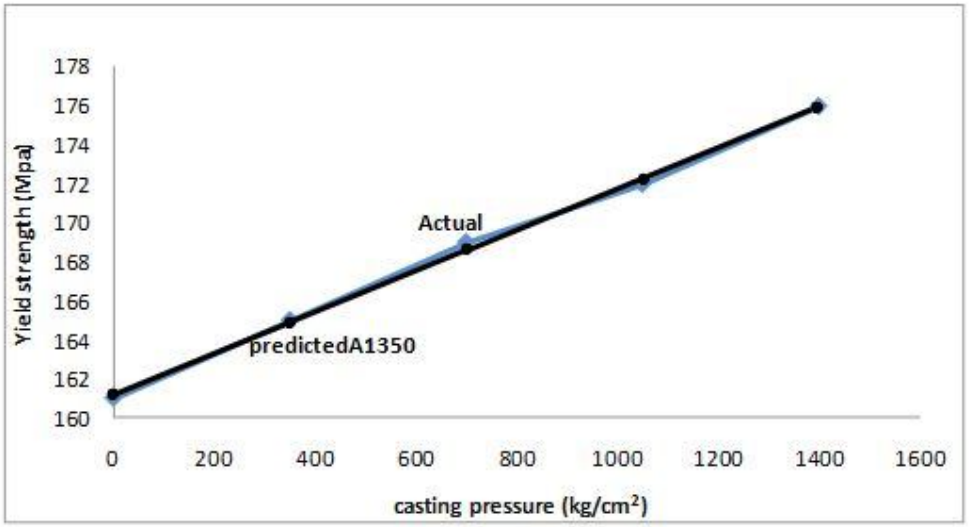


Figure 4.6: Experimental and Predicted Plots of Yield strength vs pressure of A380

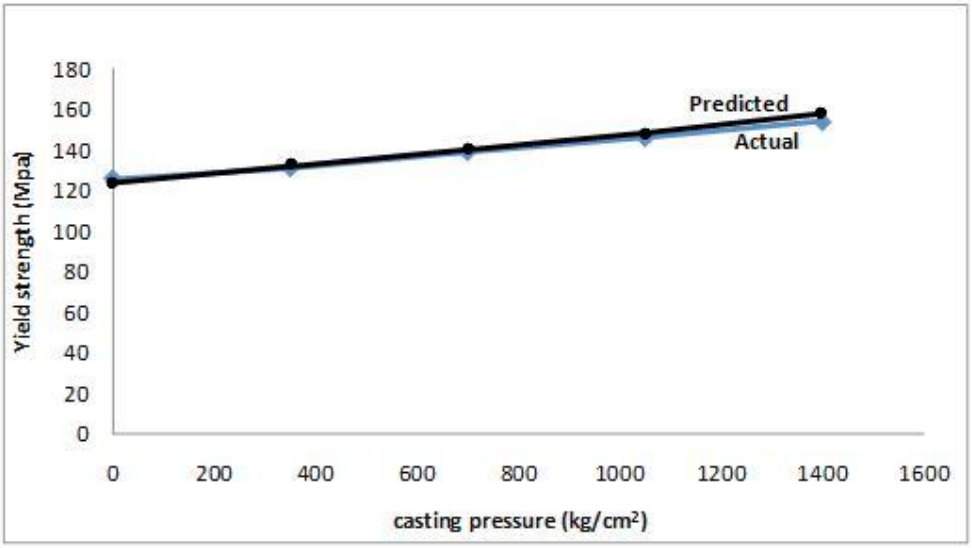


Figure 4.7: Experimental and Predicted Plots of Yield strength vs pressure of A1350

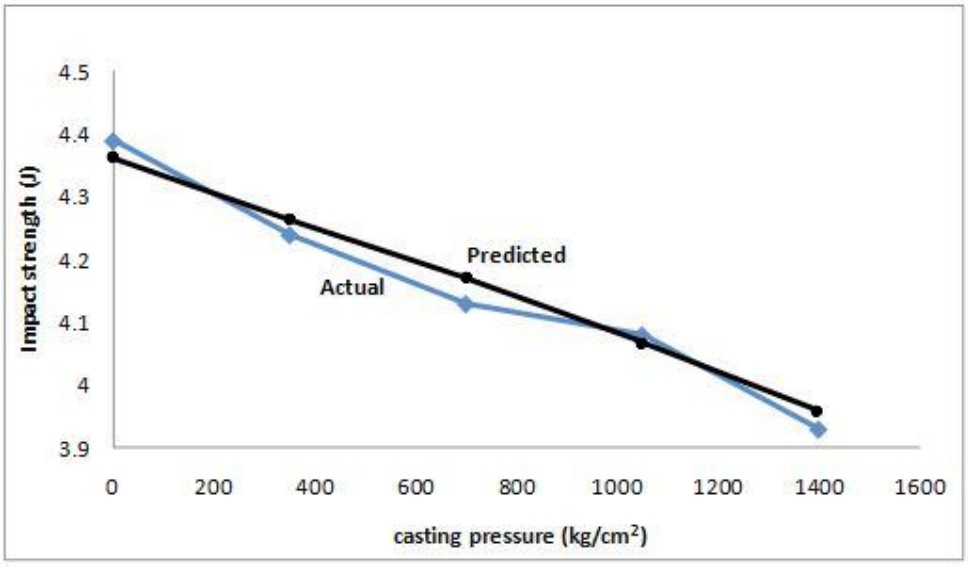


Figure 4.8: Experimental and Predicted Plots of Impact Strength vs Pressure of A380

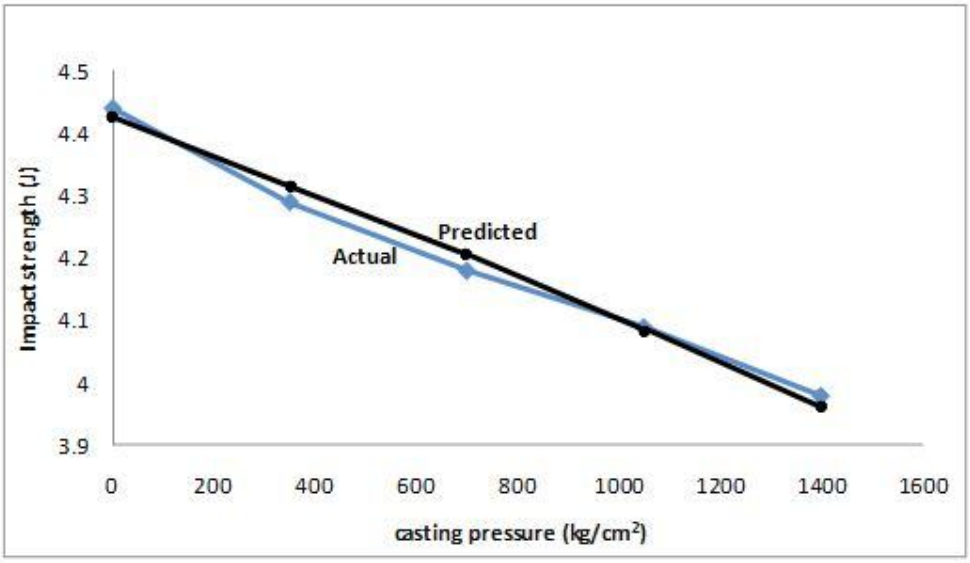


Figure 4.9:Experimental and Predicted Plots of Impact Strength vs Pressure ofA1350

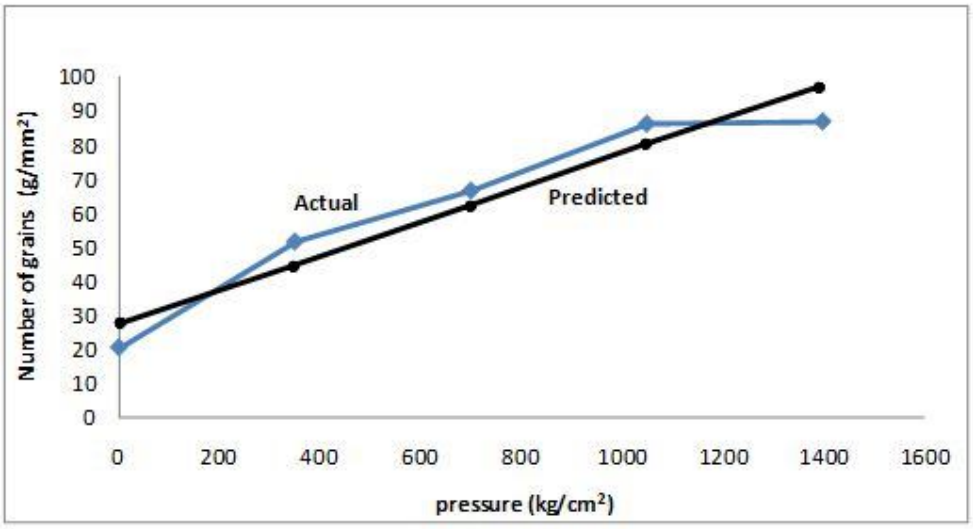


Figure 4.10: Experimental and Predicted Plots of Number of grains vs Pressure of A380

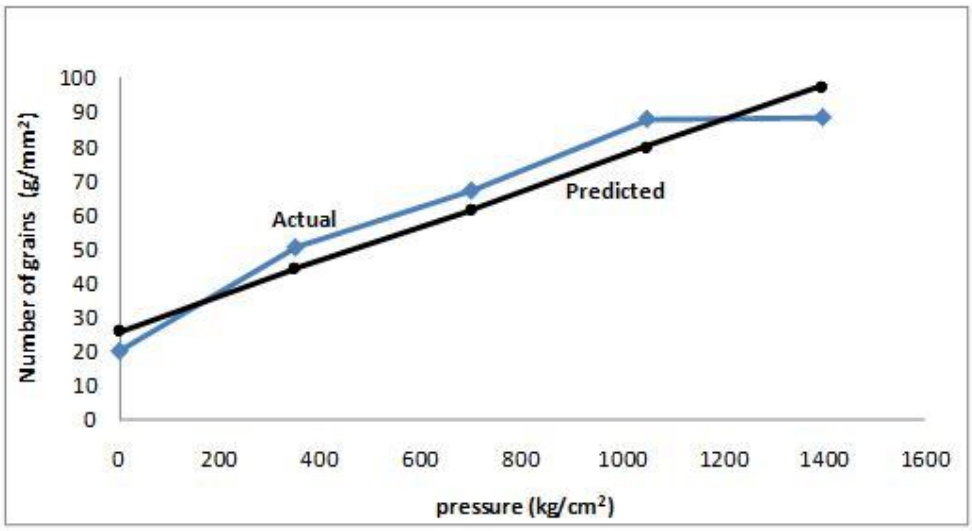


Figure 4.11: Experimental and Predicted Plots of Number of grains vs Pressure of A1350

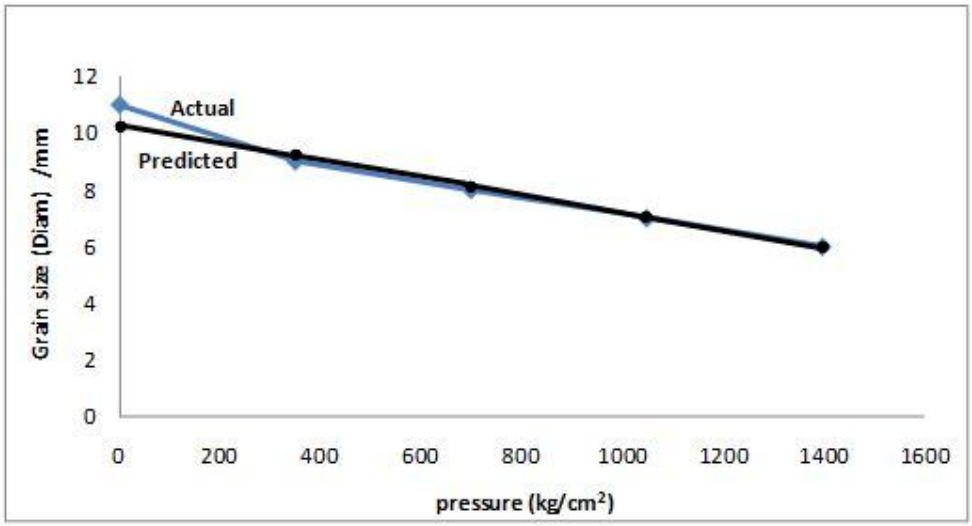


Figure 4.12: Experimental and predicted Plots of Grain Size vs Pressure of A380

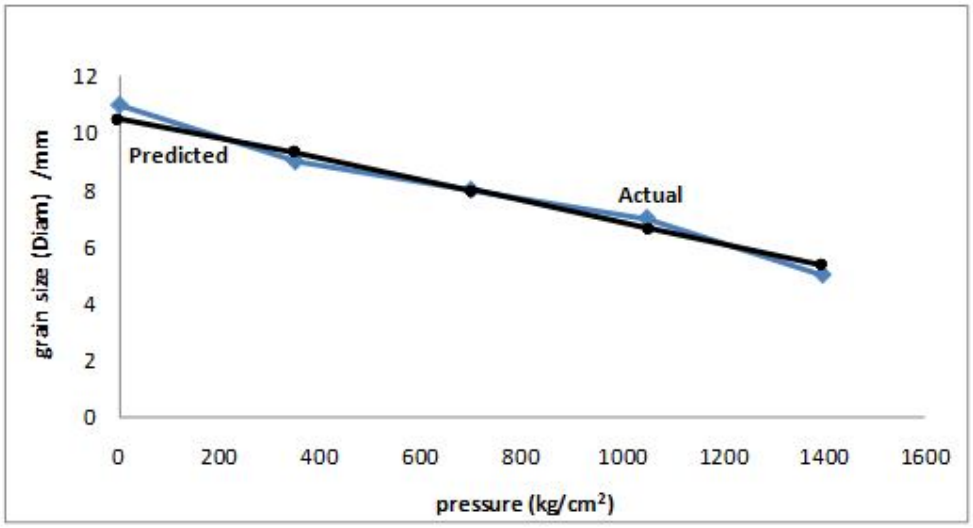


Figure 4.13: Experimental and predicted Plots of Grain Size vs Pressure of A1350

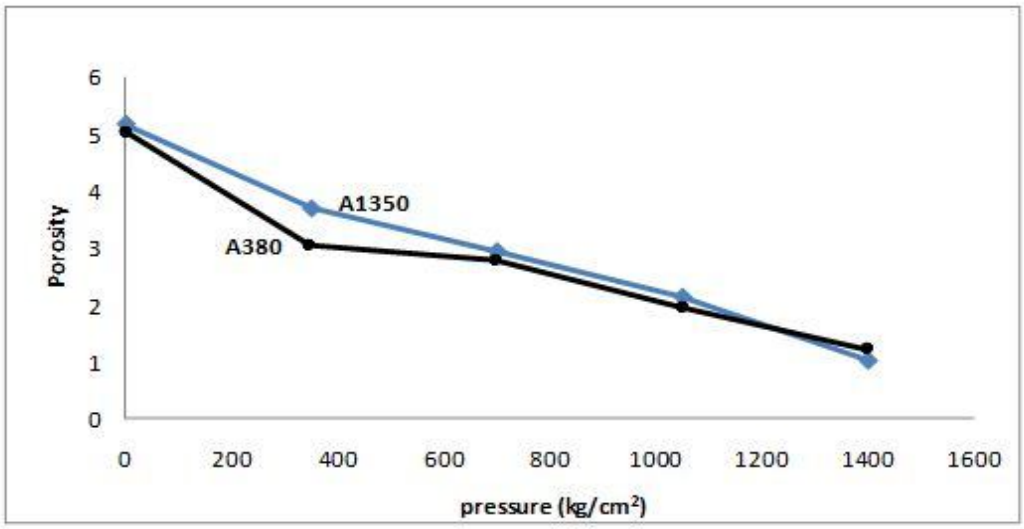


Figure 4.14: Predicted Porosity vs Pressure Plots of A380 and A1350

4.2 Discussions

4.2.1 HARDNESS

The results for the experiments were used to plot hardness - pressure graphs for both alloys (figures 4.1 and 4.2). The results obtained show that as hardness increased (even if not significantly), percentage elongation decreased (figure 4.5) with applied pressure in both alloys about 10 percent increase as pressure was raised from 350 to 1400kg/cm^2 similar to earlier work carried out by Chiang et al (2008) and Li et al (2003). Also the model that was fitted to the experimental data showed linear relationship with the actual data in view of the small error generated by them.

4.2.1.1 REGRESSION MODEL FOR HARDNESS

In the regression model, P represents pressure (0, 350, 700, 1050 and 1400 kg/ cm^2), where 76.2 and 76.8 were the constant terms present in the equations for A380 and A1350 alloys respectively. The regression model is:

$$\text{Hardness}_{(A380)} = 76.2 + 0.006\,P \quad \ldots\ldots\ldots\ldots\ldots\ldots\ldots\ldots\ldots\ldots (7)$$

The root mean square error was found to be RMSE = 0.46

$$\text{Hardness}_{(A1350)} = 76.8 + 0.062\,P \quad \ldots\ldots\ldots\ldots\ldots\ldots\ldots\ldots\ldots\ldots (8)$$

The root mean square error was found to be RMSE = 0.28

4.2.2 TENSILE TEST

The results of the tensile tests obtained for both alloys at various applied pressures were used to plot Tensile strength - Pressure graphs for both alloys as presented in figures 4.3 and 4.4. The results showed that for both alloys, tensile strength increased with applied pressure similar to works by Li et al (2003). Also the model that was fitted to the experimental data showed linear relationship with the actual data in view of the small error generated by them.

4.2.2.1 REGRESSION MODEL FOR TENSILE STRENGTH

In the regression model, P represents pressure (0, 350, 700, 1050 and 1400 kg/ cm^2), where 300.2 and 282.4 were the constant terms present in the equations for A380 and A1350 alloys respectively.

The regression model is:

$$\text{Tensile strength}_{(A380)} = 300.2 + 0.026\ P \quad \ldots\ldots\ldots\ldots\ldots\ldots\ldots\ldots\ldots\ldots\ (9)$$

The root mean square error was found to be RMSE = 2.67

$$\text{Tensile strength}_{(A1350)} = 282.4 + 0.014\ P \quad \ldots\ldots\ldots\ldots\ldots\ldots\ldots\ldots\ldots\ldots\ (10)$$

The root mean square error was found to be RMSE = 1.41

4.2.3 YIELD STRENGTH

The yield strength obtained from the tensile tests of the samples of both alloys was used to plot graphs of yield strength – pressure as seen in figures 4.6 and 4.7. The results also show that casting pressure had a similar effect on the yield stress as it did to the tensile strength for both alloys similar to those obtained by Li et al (2003). Also the model that was fitted to the experimental data showed linear relationship with the actual data in view of the small error generated by them.

.

4.2.3.1 REGRESSION MODEL FOR YIELD STRENGTH

In the regression model, P represents pressure (0, 350, 700, 1050 and 1400 kg/ cm^2), where 161.2 and 125 were the constant terms present in the equations for A380 and A1350 alloys respectively.

The regression model is:

$$\text{Yield strength}_{(A380)} = 161.2 + 0.010\ P \quad \ldots\ldots\ldots\ldots\ldots\ldots\ldots\ldots\ldots\ldots\ (11)$$

The root mean square error was found to be RMSE = 0.06

$$\text{Yield strength}_{(A1350)} = 125 + 0.020\ P \quad \ldots\ldots\ldots\ldots\ldots\ldots\ldots\ldots\ldots\ldots\ (12)$$

The root mean square error was found to be RMSE = 0.50

4.2.4 IMPACT STRENGTH

The impact energy absorbed before the material breaks are obtained from the scale on the testing machine and the results obtained were used to plot impact strength – pressure graphs of both alloys as seen in figures 4.8 and 4.9. The results also show that impact strength decreased with applied pressure in both alloys similar to works by Chiang et al [2008] and Li et al [2003]. Also the model that was fitted to the experimental data showed linear relationship with the actual data in view of the small error generated by them.

4.2.4.1 REGRESSION MODEL FOR IMPACT STRENGTH

In the regression model, P represents pressure (0, 350, 700, 1050 and 1400 kg/ cm^2), where 4.37 and 4.42 were the constant terms present in the equations for A380 and A1350 alloys respectively.

The regression model is:

$$\text{Impact strength}_{(A380)} = 4.37 - 0.0003\ P \quad \ldots\ldots\ldots\ldots\ldots\ldots\ldots\ldots\ldots\ldots\ (13)$$

The root mean square error was found to be MSE = 0.0006

Impact strength $_{(A1350)}$ = 4.42 ─ 0.00032 P ……. (14)

The root mean square error was found to be MSE = 0.00024

4.3 MICROSTRUCTURE

Specimen of 20 x 10 x 4mm were cut from each sample of both alloys and the number of grains and grain sizes were determined using the fully automated metallurgical microscope available at metallurgy laboratory at the Federal University of Technology, Minna which does automatic image analysis and measures grain size and number of grains of the specimen.

4.3.1 NUMBER OF GRAINS

The number of grains were determined and used to plot number of grains – pressure graphs as presented in figures 4.10 and 4.11. The results show an increase in the number of grains with applied pressure for both alloys in a similar manner. These results are similar with works by Ying-hui et al (2009). Also the model that was fitted to the experimental data showed linear relationship with the actual data in view of the small error generated by them also.

4.3.1.1 REGRESSION MODEL FOR NUMBER OF GRAINS

In the regression model, P represents pressure (0, 350, 700, 1050 and 1400 kg/cm2), where 28.726 and 28.078 were the constant terms present in the equations for A380 and A1350 alloys respectively.

The regression model is:

Number of grains $_{(A380)}$ = 28.726 + 0.048 P ……. (15)

The root mean square error was found to be MSE = 7.35

Number of grains $_{(A1350)}$ = 28.018 + 0.049 P ……. (16)

The root mean square error was found to be MSE = 6.86

4.3.2 GRAIN SIZE

The average grain size of the samples of both alloys per square area were recorded and was used to plot grain size-pressure graphs of both alloys as presented in figures 4.12 and 4.13. The result shows finer grain sizes with increase in applied pressure for both alloys as bigger grain sizes were obtained as pressure decreased in the casting process similar to works by Ying-hui et al (2009). Also the model that was fitted to the experimental data showed linear relationship with the actual data in view of the small error generated by them.

4.3.2.1 REGRESSION MODEL FOR GRAIN SIZE

In the regression model, P represents pressure (0, 350, 700, 1050 and 1400 kg/cm2), where 10.6 and 10.8 were the constant terms present in the equations for A380 and A1350 alloys respectively.

The regression model is:

$$\text{Grain Size}_{(A380)} = 10.6 - 0.00343P \quad \ldots\ldots\ldots\ldots\ldots\ldots\ldots\ldots\ldots\ldots (17)$$

The root mean square error was found to be MSE = 0.28

$$\text{Grain Size}_{(A1350)} = 10.8 - 0.004P \quad \ldots\ldots\ldots\ldots\ldots\ldots\ldots\ldots\ldots\ldots (18)$$

The root mean square error was found to be MSE = 0.28

4.3.3 POROSITY MEASUREMENT (Regression Model)

From the results obtained for the grain size and number of grains from the samples of both alloys, simple analogy was deduced and porosity levels predicted in relation to the grain size

and number of grains of the samples at the various pressures of the cast samples as seen in tables 4.1 and 4.2 and the results obtained were used to plot porosity – pressure graphs of both alloys as shown in figure 4.14. The relation shows low porosity levels obtained with applied pressure and higher porosity levels in the low pressure samples. The multiple regression equation was used. In the regression model, Y represents porosity level, X_1 represents grain size (6,7,8,9,11) for A380 and (5,7,8,9,11) for A1350 and X_2 represents number of grains (20.31,51.56,66.63,86.36,87.05) for A380 and (20.19,50.48,67.08,88.02,88.52) for A1350, where -2.80957 and -0.69451 were the constant terms present in the equations for A380 and A1350 alloys.

Where Y = porosity, X_1 = grain size and X2 = number of grains

The regression model is:

$$Y_{(A380)} = -2.80957 + 0.74067\,X_1 - 0.0042308\,X_2 \quad \ldots\ldots\ldots\ldots\ldots\ldots\ldots\ldots\ldots (19)$$

$$Y_{(A1350)} = -0.69451 + 0.55546\,X_1 - 0.011919\,X_2 \quad \ldots\ldots\ldots\ldots\ldots\ldots\ldots\ldots\ldots (20)$$

Table 4.1: A380 Predictor Coefficient Table for Porosity level

Pressure	0	350	700	1050	1400
(x_1)	11	9	8	7	6
(x_2)	20.31	51.56	66.63	86.36	87.05
Constant	−2.80957	−2.80957	−2.80957	−2.80957	−2.80957
X_1 (0.74067)	8.14737	6.6603	5.92536	5.18469	4.44402
X_2 (−0.0042308)	−0.085928	−0.21814	−0.281898	−0.36537	−0.36829
Porosity	5.10450	2.90853	2.833892	2.00975	1.26616

Table 4.2: A1350 Predictor Coefficient Table for Porosity level

Pressure	0	350	700	1050	1400
(x_1)	11	9	8	7	5
(x_2)	20.19	50.48	67.08	88.02	88.52
Constant	─0.69451	─0.69451	─0.69451	─0.69451	─0.69451
X_1 (0.55546)	6.11006	4.99914	4.44368	3.88822	2.7773
X_2 (─0.011919)	─0.24065	─0.60167	─0.79953	─ 1.04911	─ 1.05507
Porosity	5.1749	3.70296	2.94964	2.1446	1.02772

4.4 MICROSTRUCTURE ANALYSIS

4.4.1 Microstructural Chacterization

The microstructures of the samples of both alloys at different pressures consisted of a primary α phase, peritectic β phase and hypoeutectic (β+η+ε), where α phases solidified as coarse grains (Figures.4.17 and 4.22) The primary α phases became finer in higher pressure (seen in Figures 4.16 and 4.21) and with the increase of pressure, the microstructure of both alloys became finer, and even primary α phases appeared as nodular when the pressure reached 1400 kg/cm^2 (seen in Figures 4.15 and 4.20).

In the lower pressure samples, scanty grains were seen and they were not homogeneously distributed (Figures 4.19 and 4.24), also the eutectic structure (β+η+ε) was not found in the samples at 1400 kg/cm^2 , while the (η+ε) phases appeared between grains (Figures 4.15 and 4.20). In the solidification process of both alloys, the primary phase α precipitates first from liquid phase and then the hypoeutectic reaction follows. However, at high pressure, the degree of these two reactions becomes greater due to the fact that the eutectic point in both alloys moves to the direction of rich Al, thus the quantity of remaining liquid phase is reduced greatly. On the other hand, because the melting points of both alloys are elevated at high pressure, the degree of super-cooling increases, thus the nucleate rate of primary reaction increases largely during solidifying. This is also the reason for microstructure refining, In addition, the remaining phase is in deep super-cooling state when temperature is dropped to the eutectic point.

Therefore, the improvement of mechanical properties is attributed to eliminating of micro-pores in the alloys caused by higher pressure. On the other hand, it is because of the microstructure refining as the applied pressure is increased as seen below (figures 4.15, 4.16, 4.20 and 4.21) that increased tensile strength and hardness are attributed to. From the above

results, it can be deduced that the eutectic reaction was restrained while the primary reaction was promoted in both alloys at higher pressure similar to works by Ming et al (2007), Li et al (1997) and Ying-hui et al (2009)

4.4.2 MICROSTRUCTURE AND MICROGRAPH OF A380 SAMPLES

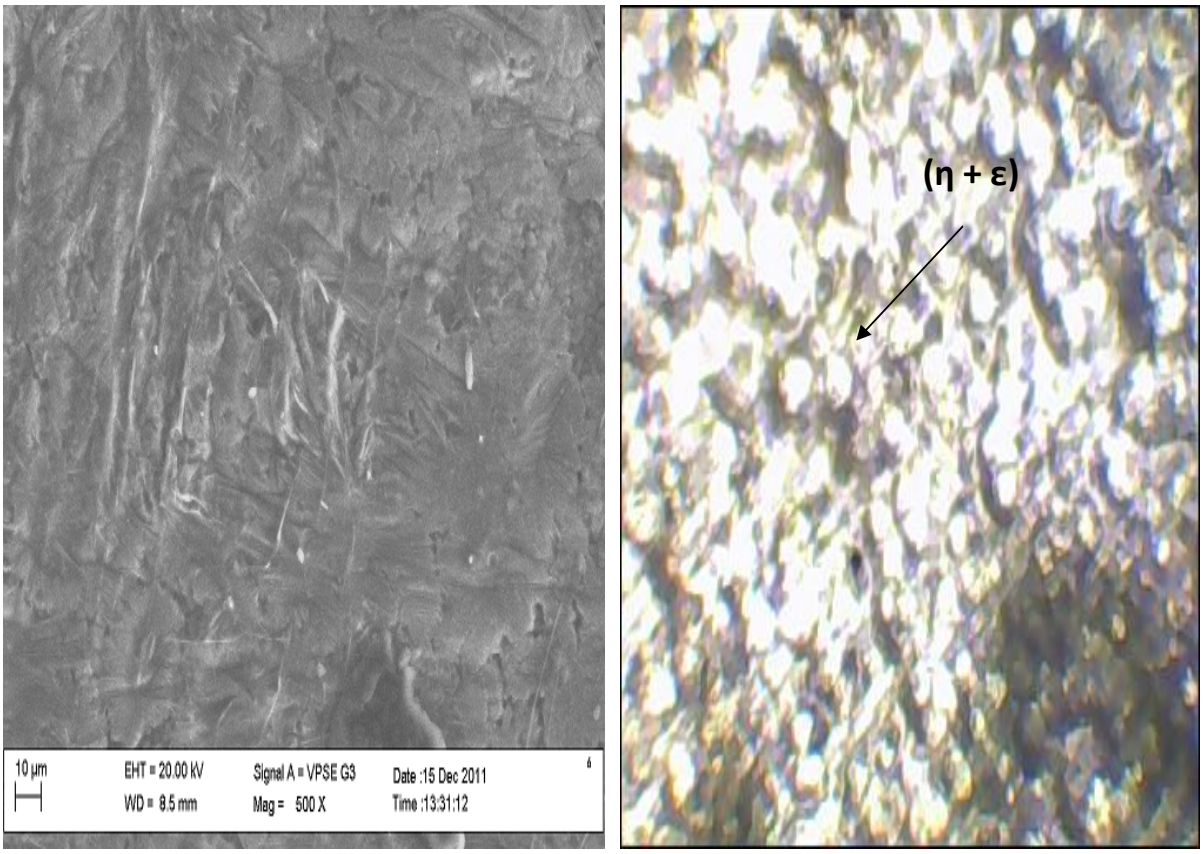


Figure 4.15 : Microstructure and Micrograph of sample 1 of A380 with Injection pressure of 1400 Kg/cm2

From figure 4.15 of the microstructure and micrograph of the above sample, the grains were clearly seen, also the spherical dimples characteristics of grain type were clearly seen and almost 95 percent of grains occupy the micrograph showing fine grain sizes. The much concentrated grains were cohesively arranged and evenly distributed due to good compatibility of the grain structure which is absolutely, evenly distributed in an attractive manner and perfectly embedded with one another. The improvement of mechanical properties is attributed to eliminating of micro-pores in the alloy caused by applied pressure and this is because of the microstructure refining as the applied pressure is increased as mentioned above.

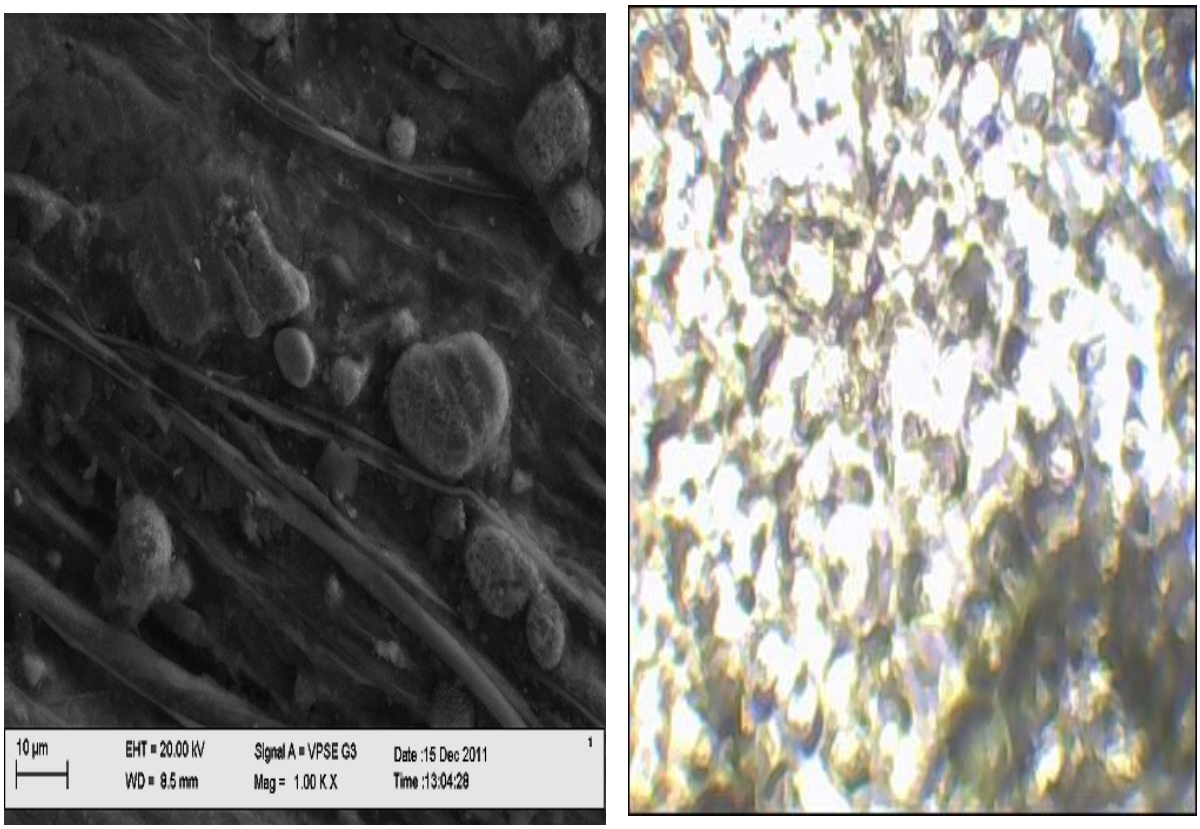


Figure 4.16 : microstructure and Micrograph of sample 2 of A380 with Injection pressure of 1050 Kg/cm2

In figure 4.16, the micrograph shows spherical dimples characteristics of grain types which are still shown occupying almost 85 percent the micrograph showing also fine grain sizes and also the much concentrated grains were cohesively arranged and evenly distributed also due to good compatibility of the grain structures. The improvement of mechanical properties is attributed to eliminating of micro-pores in the alloy caused by applied pressure.

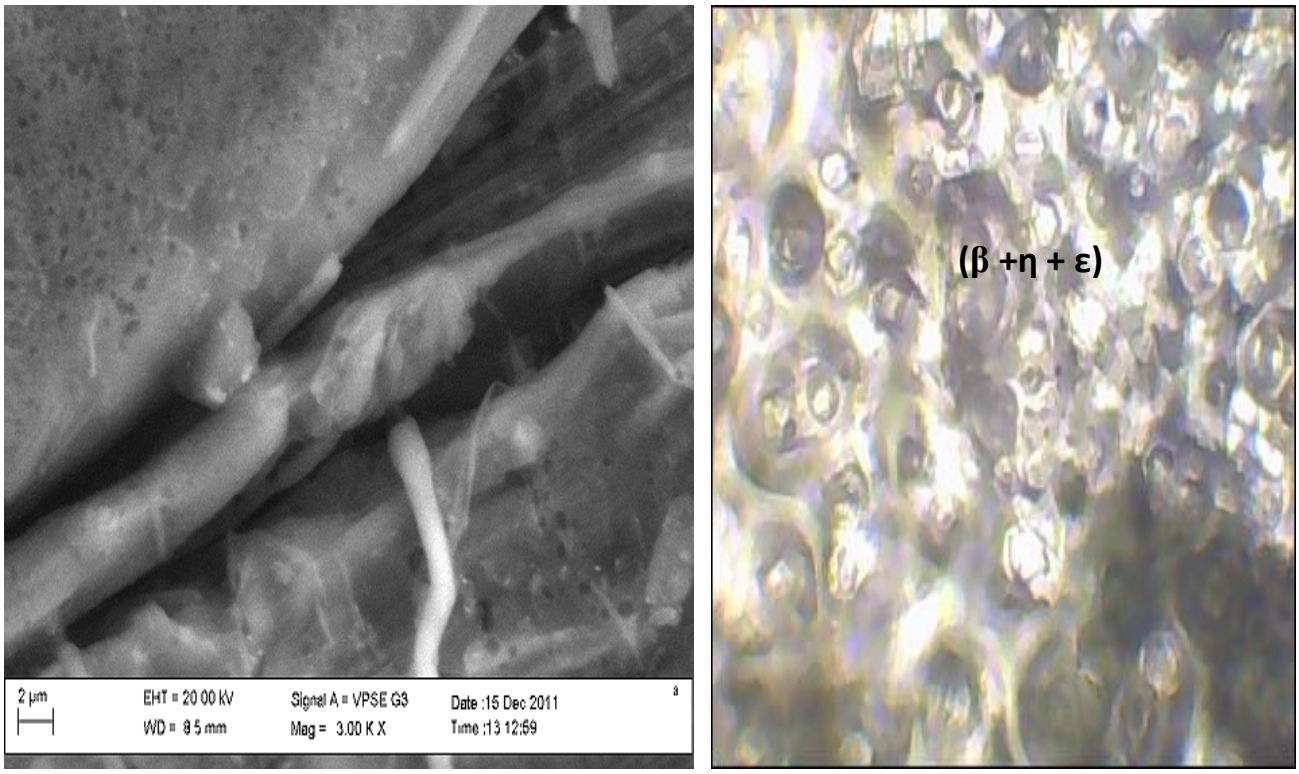


Figure 4.17 : Microstructure and Micrograph sample 3 of A380 with Injection pressure of 700 Kg/cm2

In figure 4.17, the microstructure shows the much concentrated grains cohesively arranged and evenly distributed, also the spherical dimples characteristics of grain type are still shown and almost 75 percent of grains occupy the micrograph showing not very fine grains.

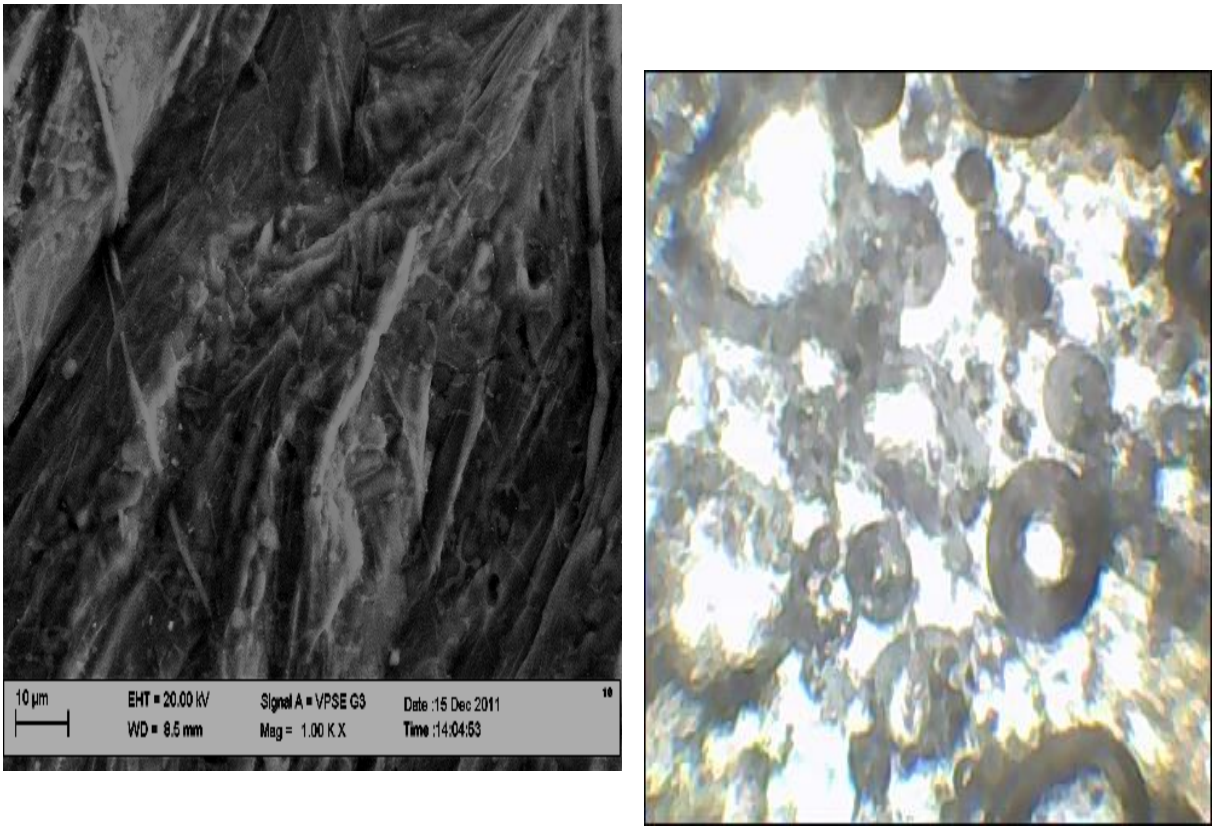


Figure 4.18 : Microstructure and Micrograph of sample 4 of A380 with Injection pressure of 350 Kg/cm2

In figure 4.18, the micrograph shows spherical dimples characteristic of grain type and almost 70 percent of grains occupy the micrograph showing big grain sizes. It was also clearly shown that the grains were scanty because of bigger grain sizes that depict porosity susceptibility over time.

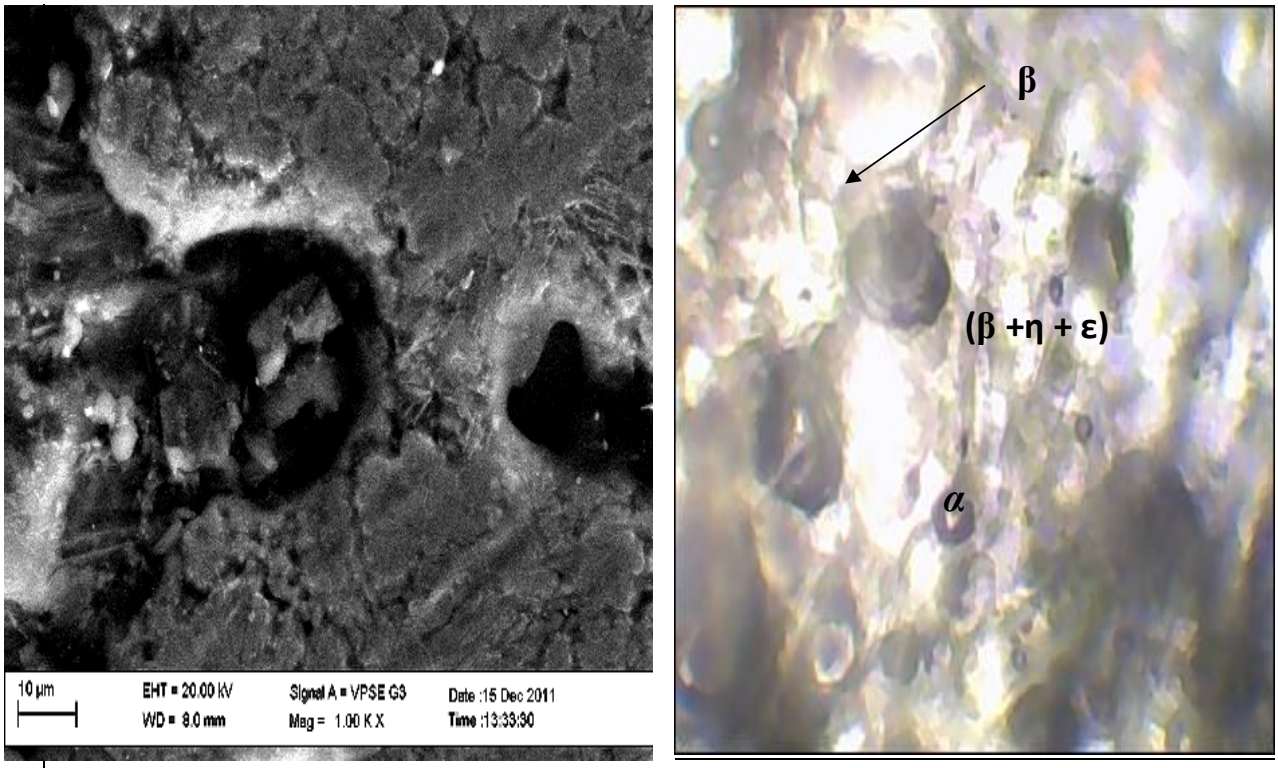


Figure 4.19: Microstructure and Micrograph of sample 5 of A380 with Injection pressure of 0 Kg/cm2

From the microstructure and micrograph of figure 4.19, it is seen that the grains are very scanty, also the region occupied by grains was less than 40 per cent and shows big grain sizes. The micrograph also shows deformation that is worsened and the degree of deformation so great. The microstructure clearly shows obvious porosity in the sample that solidified at low pressure.

4.4.3 MICROSTRUCTURE AND MICROGRAPH OF A1350 SAMPLES

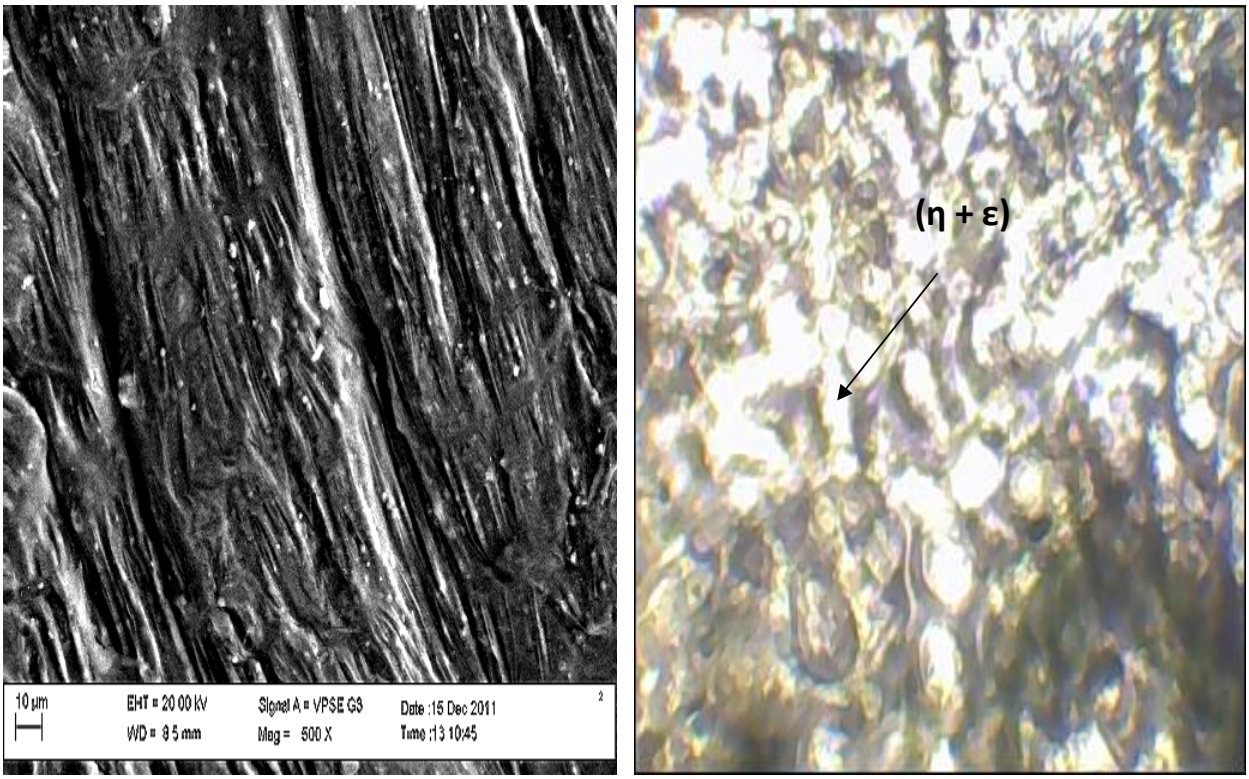


Figure 4.20: Microstructure and Micrograph of sample 1 of A1350 with Injection pressure of 1400 Kg/cm2

The microstructure of figure 4.20 shows fine grain structures that produced elongated pattern and the grains were finely and cohesively arranged and 95 percent or more of grains occupy the micrograph showing finer grain sizes, also the micrograph shows ductile aluminum of transgranular surface due to good compatibility of the grain structures which is absolutely, evenly distributed in an attractive manner and perfectly embedded with one another. Also the improvement of mechanical properties is attributed to eliminating of micro-pores in the alloy caused by applied pressure and this is because of the microstructure refining as the applied pressure is increased as mentioned above.

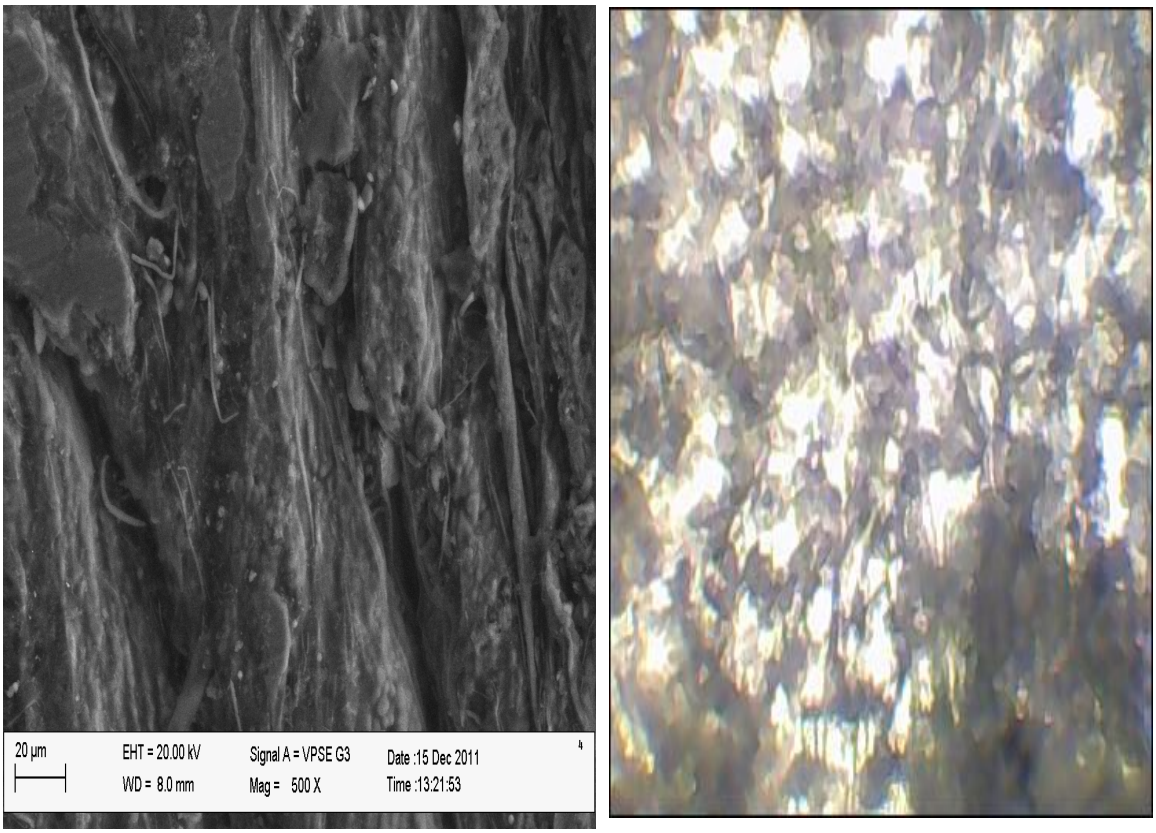


Figure 4.21: Microstructure and Micrograph of sample 2 of A1350 with Injection pressure of 1050 Kg/cm2

In figure 4.21, the micrograph shows that the grains are cohesively arranged and spherical dimples characteristics of grain type were seen and almost 85 percent of grains occupy the micrograph showing fine grain sizes also. The much seen grains were evenly distributed across the microstructure, due to good compatibility of the grain structures which is embedded with one another. The improvement of mechanical properties is attributed to eliminating of micro-pores in the alloy caused by applied pressure.

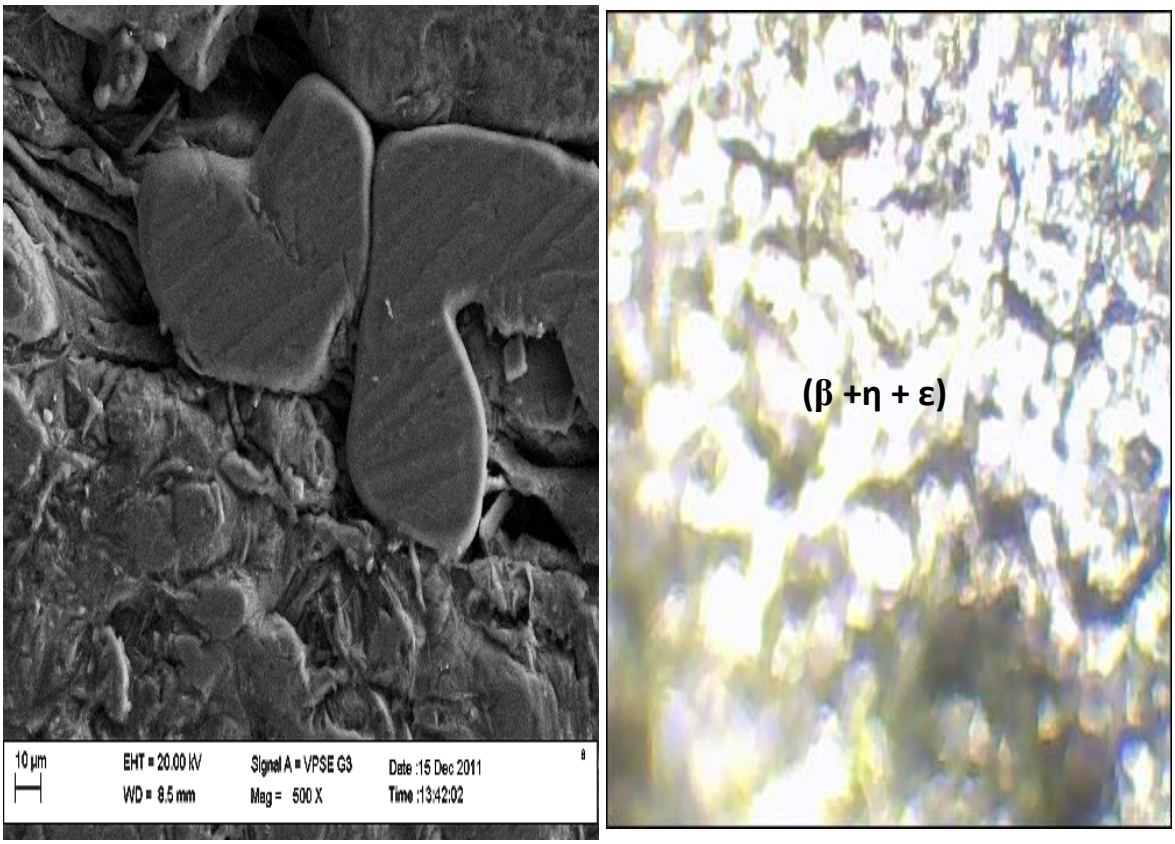


Figure 4.22: Microstructure and Micrograph of sample 3 of A1350 with Injection pressure of 700 Kg/cm2

In fig 4.22, the microstructure shows that the grains are cohesively arranged and appear in a parabolic-shaped dimple characteristic appearance of the grains. The micrograph shows a ductile aluminum of a transgranular fracture surface. It also shows that almost 70 percent of grains occupy the micrograph, but leaving spaces which obviously show not very fine grains.

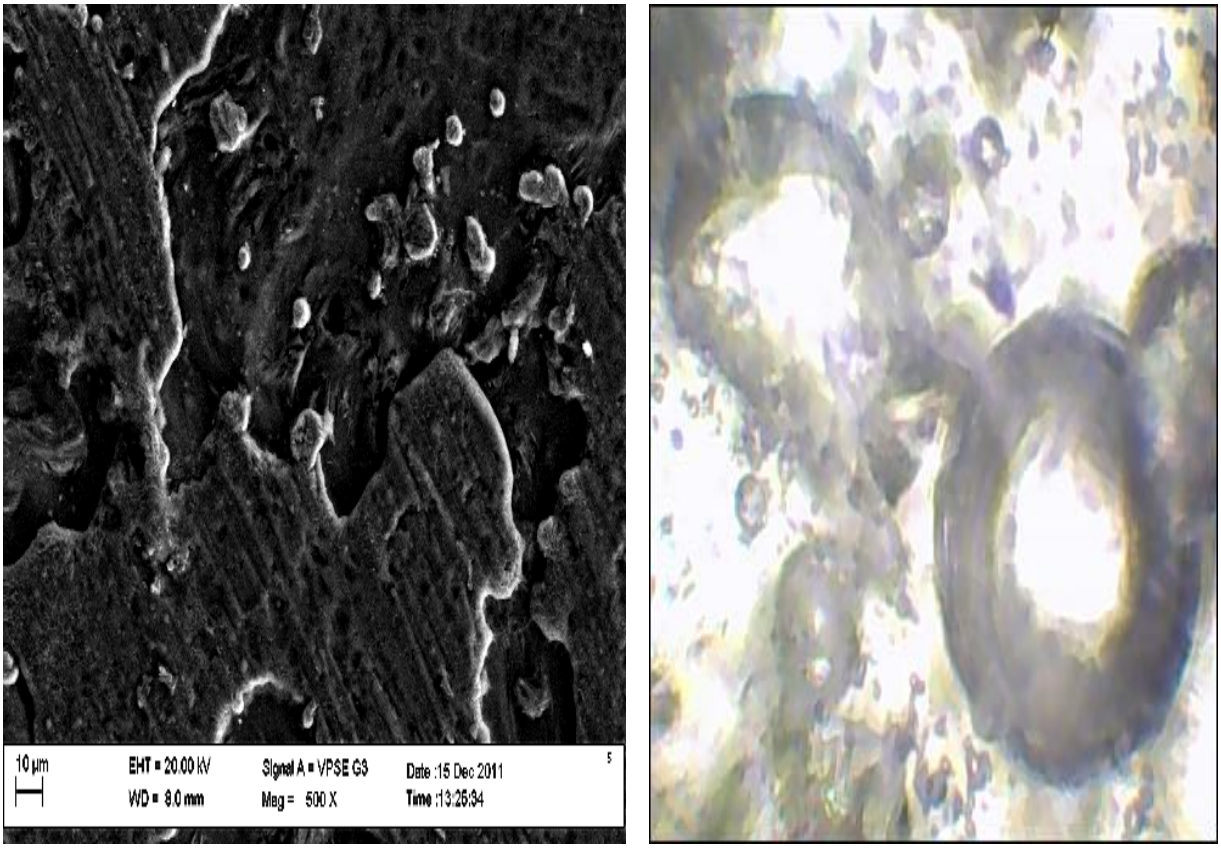


Figure 4.23: Microstructure and Micrograph of sample 4 of A1350 with Injection pressure of 350 Kg/cm2

In fig 4.23, the microstructure and micrograph shows that grains are cohesively arranged and appear in parabolic–shaped dimple characteristics. Fine grains were seen. Not many grains appeared across the micrograph and almost 60 percent or fewer grains occupy the microstructure leaving visible spaces that show big grain sizes that indicate porosity susceptibility over time.

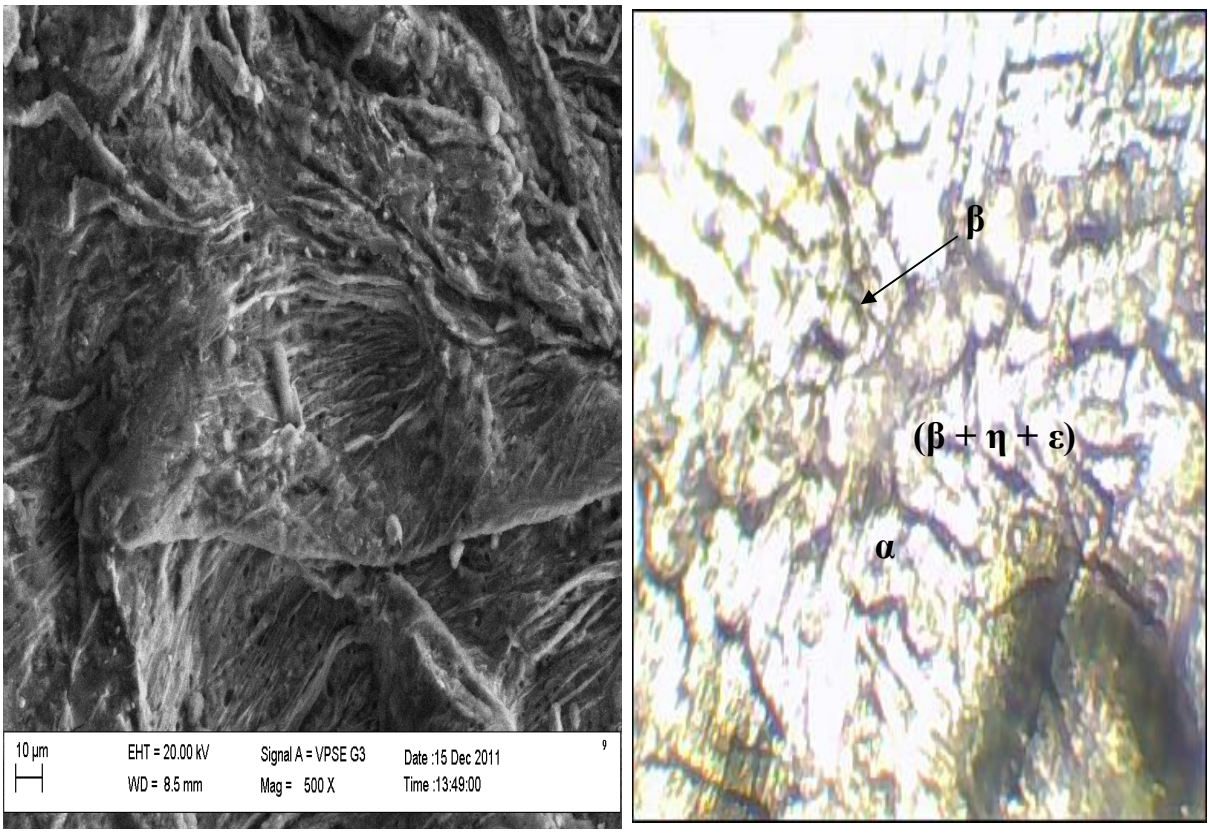


Figure 4.24: Microstructure and Micrograph of sample5 of A1350 with Injection pressure of 0 Kg/cm2

From the microstructure and micrograph of fig 4.24, it is seen that the grains are very scanty and the regions at which they occupy are about 30 percent of the micrograph. The microstructure and micrograph also show deformation that is worsened and the degree of deformation so great. The grains clearly show no morphology that is obvious, probably due to low pressure. The microstructure clearly shows obvious porosity in the sample that solidified at low pressure.

CHAPTER 5

CONCLUSIONS AND RECOMMENDATIONS

5.1 CONCLUSIONS

From the results of this research, the following conclusions can be drawn:

i. The hardness of both alloys increased and percentage elongation decreased with applied pressure. Also the model that was fitted to the experimental data showed linear relationship with the actual data in view of the small error generated by them.

ii. Tensile and yield strengths of both alloys also increased with applied pressure. Also the model that was fitted to the experimental data showed linear relationship with the actual data in view of the small error generated by them.

iii. The impact strengths of both alloys were observed to vary in similar manner across the different applied pressures in the casting process as the impact strengths of both alloys decreased as hardness increased with applied pressure. Also the model that was fitted to the experimental data showed linear relationship with the actual data in view of the small error generated by them

iv. The number of grains increased with applied pressure for both alloys. Also the grains became finer with applied pressure for both alloys. Also the model that was fitted to the experimental data showed linear relationship with the actual data in view of the small error generated by them.

v. The microstructures obtained of the samples of both alloys at different pressures also showed that at applied pressure of 1400kg/cm^2, the eutectic reactions were restrained,

and the final solidified structure was (η+ε) phases instead of eutectic phase (β+η+ε) signifying the effect of applied pressure, also the primary aluminum reaction (α) was promoted in the samples that solidified at 1400kg/cm^2 and fine microstructures were obtained .

vi. The micrographs showed the different morphologies that were distributed across the samples of both alloys under the different applied pressures. The fine grains which were homogenously distributed on micrographs of both alloys at 1400 kg/cm^2 can effectively block the movement of dislocations, thus increase the strength and plasticity of both alloys.

vii. Microstructures of the samples of both alloys showed structural changes (granular, lamellar, coarse e.t.c) due to pressure variation.

viii. Porosity susceptibility in the samples of both alloys decreased with applied pressures due to fine grains and more numbers of grains as no pore was seen on the micrographs and microstructures of samples that solidified at pressures of 1400kg/cm^2 in both alloys.

ix. For all the models developed, a close relationship with the experimental results were underlying in view of the small errors generated by them and can be used to predict the experimental values of this research.

5.2 RECOMMENDATIONS FOR FURTHER WORK

In the research work, A380 alloy and A1350 alloy have been studied. Other alloys should also be investigated for different reasons:

i. Effect of pouring temperature on grain refinement and mechanical properties of die cast A360 and aluminum magnesium alloy.

ii. Effects of various cooling media should also be carried out on mechanical properties of die cast aluminum alloys.

iii. Pressure effects should be carried out on porosity and grain refinement of die cast alloys.

iv. Effects of other input parameters on the microstructure of die castings.

v. The influence of pressure on the cost of energy consumed in the process

5.3 Contributions of the research work to knowledge

The results of this research can contribute to improving the quality of aluminum die castings by:

i. Using the model equations to predict variable responses to experimental values of the mechanical properties and other properties and can be used to predict future variable responses in future work.

ii. Decrease in porosity

iii. Increase in strength evidenced by mechanical properties

iv. Higher quality due to reduced grain size and more number of grains

v. Expected assurance that die castings are less prone to rejection and are of higher standard of soundness through microstructure refining.

References

Adler, L., Nagy, P. B., Rypien, D. V., and Rose, J. H., (1989): Ultrasonic Evaluation of Porosity in Aluminium Cast Materials, Ohio State University, Columbus, OHIO, USA.

Ambardar, R., Jayakumar, T., Pathak, S. D., and Prabhakar, O., (1996) : Effect of Surface Roughness on Ultrasonic Echo Amplitude in Aluminium-Copper alloy Castings in the 14th World Conference on Non Destructive Testing, New Delhi, india, vol. 2, pp. 981-984.

An-ming, L., Hai-rui, W., (2008): Effect of Silicon and Manganese on Mechanical Properties and Microstructure of As-Cast ZA-27 alloy [J]. Foundry, 57(6): 608−610. (in Chinese)

Anon, (1978): Aluminium Technology Book 6: Casting Aluminium, Canberra: Aluminium Development Council of Australia Ltd.

Aleksandr, A.S., ĭMikhaĭlov, A.P., (2002): Principles of Mathematical Modeling: Ideas, Methods, Examples Volume 3 of Numerical Insights, Taylor and Francis publishers, Moscow.

Allen, D. M., (1971): Mean Square Error of Prediction as a Criterion for Selecting Variables, Technometrics, 13, 469–475.

Aris, Rutherford, (1994): Mathematical Modeling Techniques, New York.

ASM handbook volume 15, casting (2008 Edition).

Aweda, J.O., (2006): Temperature Distribution and Properties in Squeeze Casting of Aluminium, Ph.D. Thesis, Mechanical Engineering Department, University of Ilorin, Ilorin, nigeria.

Beckhoff, B., Kanngießer, B., Langhoff, N., Wedell, R., Wolff, H., (2006): Handbook of Practical X-Ray Fluorescence Analysis.

Brown, J.R., (1999): Non-Ferrous Foundry Man's Handbook, Butterworth, Oxford.

Campbell, J., Harding, R.A., (2000): Casting Technology in TALAT 2.0 CD─ROM, EAA, Bruxelles.

Campbell, J., (1999) : The 10 Casting Rules: Guidelines for the reliable production of reliable castings; A draft process specification, 1st International Conference on gating, Filling and Feeding of Aluminum Castings, American Foundry Men's Society, Nashville, TN, Oct. 11-13.

Cha, P.D., Rosenberg, J.J., and Dym, C.L., (2000) : Fundamentals of Modeling and Analyzing Engineering Systems, Cambridge University Press,New York.

Chen-xi, L., Jing-chao, S. , Na, X., Liang, C., Yan-hua, B., Rong-de, L., (2005) : Research on the Squeeze Cast Technology of the Castings with Large Ratio of Height to Thickness [J]. China Foundry, 2(4): 264−267.

Chiang Ko-Ta, Liu, Nun-Ming and Tsai Te-Chang., (2008): Modeling and Analysis of the Effect of Processing Parameters on the Performance Characteristics in the High Pressure Die Casting Process of Al-Sl alloys, Int J Adv Manuf Technol 41:1076-1084, Springer-Verlag London.

Cook, R. D., (1979) : Influential Observations in Linear Regression, Journal of the American Statistical Association, 74, 169–174.

Dahle, A.K., Arnberg, L. and Apelian, D., (1997): Burst Feeding and its Role in Porosity Formation during Solidification of Aluminum Foundry alloys, 101st Casting Congress, American Foundry men's Society, Seattle WA.

Dahle, A. K. and St John, D. H., (2002): Processing Via Liquid State. In: Encyclopaedia of Life Support Systems (EOLSS), Eolss Publishers. Oxford.

Daniel, L. Rubinfeld, & Peter, O. Steiner, (1983): Quantitative Methods in Antitrust Litigation, Law & Contemp. Probs.

Doehler, H., (1910): Art of and Apparatus for Casting Fluid Metal, United States Patent 973,483, United States Patent and Trademark Office, Washington D.C., 25, October 1910.

Doehler, H., (1951): Die Casting, McGraw Hill Book Company, New York.

Draper, N. and Smith, H., (1981): Applied Regression Analysis, Second Edition, New York.

Duckett, G., (1988): Quality-Whose Definition? Foundry Trade Journal, vol.163, pp. 660-661.

Hatch, J.E., (1984): Aluminum: Properties and Physical Metallurgy, American Society for Metals, Metals Park, Ohio.

(http://business.ezinemark.com/die-casting)

James, W. H., (1996): Modeling Biological Systems: Principles and Applications. Springer. pp. 186–189.

Jenkins, R., De Vries, J. L., (1973): Practical X-ray Spectrometry, Springer-Verlag.

Ji-ping, X., Wei-zhi, J., Zhi-qin, H., (2005): Squeeze Casting of Zn-Al alloy Gears with High Strength [J]. Special Casting and Nonferrous Alloys, 25(10): 637−638. (in Chinese).

Korotayev, A., Malkov, A., Khaltourina, D., (2006): Introduction to Social Macrodynamics: Compact Macromodels of the World System Growth. Moscow.

Kumar, L. (2010): Multi-Response Optimization of Process Parameters in Cold Chamber Pressure Die Casting, M.ENG thesis, Mechanical Engineering Department, Thapar University India.

Li, Rong-de, L., Zhong-ping, H., Yan-hua, B. , Qing-sheng, Z. , Hai-feng, Z. (2003): Effect of Super-High Pressure on the Non-Equilibrium Solidified Microstructure and Mechanical Properties of ZA27 alloy [J]. Foundry, 52 (3): 92−94.

Major. J., Tynelius K., and Apelian, D. (1993): A Parametric Study of Microporosity in the A356 Casting Aluminum System" AFS Trans. 101, 401-413.

Matthew S, Dargusch, A., Dourb, G., Schauer, C., Dinnis, C.M. and Savaged, G. (2006): The Influence of Pressure during Solidification of High Pressure Die Cast Aluminium Telecommunication Components, Journal of Materials Processing Technology 180. Pp.37-43.

Mikelonis, P. L. (1986): Foundry Technology. In: Quality Management Handbook, eds. Walsh, L., Wurster, R., and Kimber, R. J. Marcel Dekker. new york, pp. 753-790.

Ming, Z., Wei-wen, Z. , Hai-dong, Z. , Da-tong, Z. , Yuan-yuan, L. (2007): Effect of Pressure on Microstructures and Mechanical Properties of Al-Cu-based alloy Prepared by Squeeze Casting [J]. Transactions of Nonferrous Metals Society of China, 17(3): 496−501.

NADCA, (2010): About Die Casting, The North American Die Casting Association, archived from the original on http://www.webcitation.org/5tVCFPCyL, retrieved 2010-10-15.

Richard, W. H., Carl, R. L. Jr., and Philip, C. R. (1967): Principles of Metal Casting, New York: McGraw-Hill.

Rickards, P. J. and Wickens, M. (1994): Testing of Iron Castings, Foundry International, vol. 17, no. 4, pp. 162-166.

Sabau, A.S. and Vishvanathan, S.,(2002): Micro Porosity Prediction in Aluminum alloy Castings, Metallurgical and Materials Transactions *b Vol.33B.pp.243*.

Schleg, S., Kamicki, D.P. (2000): Guide to Casting and Molding Processes, Engineered Casting Solutions, Technical Articles.

Shu-qing, Y., Jing-pei, X., Zhong-xia, L., (2008): Effect of Al Contents on Microstructure and Wear Resistance of ZA alloy [J]. Hot Working Technology, 37(1): 10−14. (in chinese)

Sigworth, G.K., Wang, C., Huang, H. and Berry, J.T. (1994): Porosity Formation in Modified and un-Modified Al-Si alloy Castings, AFS transactions, Vol. 102, 245-261.

Street, A.C. (1990) : The Die Casting Book – 2nd Edition, Portcullis Press.

Suresh, P. (2006): Ultrasonic Inspection of Gas Porosity Defects in Aluminum Die Castings, Ph.D. thesis Mechanical Engineering Department, Swinburne University of Technology, Hawthorn, Melbourne, Australia.

Taylor, H. F., Wulff, J., and Flemings, M. C. (1959): Foundry Engineering, New York: John wiley.

Taylor, J.A. (1995): Metal-Related Castability Effects in Aluminum Foundry alloys, Cast Metals, Vol. 8, No. 4, 225-252.

Watmough, (1960): The Effects of 0, 10, 20 psi (0, 0.069, and 0.138MPa) Pressure levels on the X-ray Soundness of Sand Cast Steel Bars, Norway.

Weisberg, S. (1985): Applied Linear Regression, Second Edition. New York: John Wiley & Sons.

(www.tech/info/die-cast.com). Uploaded Jan- 6- 2011.

Yan-xia, L., Tung-wai, N. , Hai-dong, Z. , Wei-wen, Z. , Yuan-yuan, L. (2005): Microstructure and Mechanical Properties of Squeeze Cast Al-Cu alloy with Different Applied Pressure. Foundry, 54(8), 764−766. (in Chinese).

Ying-hui, W., Li Feng, H., Li-jing, Y., Bing-she, X., Munehiro, K., and Hideki, I. (2009) : Microstructure and Properties of Die Casting Components with Various Thickness made of AZ91D alloy, Journal of Materials Processing Technology 209.pp.3278-3284.

Yoshihiko, H and Soichiro, K. b. (2009): Quantitative Evaluation of Porosity in Aluminum alloy Die Castings by Fractal Analysis of Spatial Distribution of Area, Materials and Design 30.pp.1169-1173.

Yu, H. P, Zhang, F. Q, Li, R.D. (1997): Strengthening and Toughening Mechanism of ZA27 Squeeze-Cast alloy [J]. AFS Transactions, 47: 689−692.

Zhu, J.D., Cockcroft S.L., and Maijer, D.M. (2006): Modeling of Micro Porosity Formation in A356 Aluminum alloy Casting, Metallurgical and Materials Transactions A. Vol. 37A.pp.1075.

Zi-quan, L., Heng-zhi, Z., Xin-yi, L., Tao, W., (2006): Aging Microstructural Characteristics of ZA-27 alloy and SiCp/ZA-27 Composite [J]. Transactions of Nonferrous Metals Society of China, 16(1): 98−104.

APPENDIXES

Table A1: Hardness Number for A380 Samples

Injection pressure ($Kg/cm^{2)}$	A380 Sample no	Hardness (HRN)	Predicted hardness
0	1	76	76.2
350	2	79	78.3
700	3	80	80.4
1050	4	82	82.5
1400	5	85	84.6

Table A2: Hardness Number for A1350 Samples

Injection pressure ($Kg/cm^{2)}$	A1350 Sample no	Hardness (HRN)	Predicted hardness
0	1	77	76.8
350	2	79	79.0
700	3	81	81.20
1050	4	83	83.40
1400	5	86	85.60

Table A3: Tensile strength of A380 samples

Area $A_0 = 7.5 \times 10^{-5}$ m^2 **Gauge length $l_0 = 45mm$**

Injection pressure ($Kg/cm^{2)}$	Maximum Load (KN)	Tensile strength (MPa)	Extension (mm)	Elongation (%)
0	25.2	298	4.46	10.01
350	24.7	313	4.30	9.56
700	23.8	317	4.09	9.09
1050	23.5	329	3.94	8.75
1400	22.4	336	3.82	8.49

Table A4: A380 Predictor Coefficient Table for Tensile Strength

Pressure	0	350	700	1050	1400
Constant	300.2	300.2	300.2	300.2	300.2
(0.0262)P	0	9.20	18.40	27.60	36.80
Tensile Strength	300.2	309.4	318.6	327.8	337

Table A5: Tensile Strength of A1350 Samples

Area $A_0 = 7.5 \times 10^{-5}$ m^2 **Gauge length $l_0 = 45mm$**

Injection pressure ($Kg/cm^{2)}$	Maximum Load (KN)	Tensile strength (MPa)	Extension (mm)	% elongation
0	22.7	281	4.39	9.76
350	22.3	289	4.18	9.30
700	22.0	293	4.02	8.93
1050	21.7	297	4.86	8.58
1400	21.1	302	3.68	8.17

Table A6: A1350 Predictor Coefficient Table for Tensile Strength

Predictor	0	350	700	1050	1400
Constant	282.4	282.4	282.4	282.4	282.4
P(0.0142857143)	0	5.0	10.0	15.0	20.0
Tensile Strength	282.4	287.4	292.4	297.4	302.4

Table A7: Yield Strength of the A380 and A1350 Samples

Injection pressure ($Kg/cm^{2)}$	A380 Sample no	Yield strength (MPa)	A1350 Sample no	Yield strength (MPa)
0	1	161	1	126
350	2	165	2	131
700	3	169	3	139
1050	4	172	4	146
1400	5	176	5	154

Table A8: A380 Predictor Coefficient Table for Yield Strength

Pressure	0	350	700	1050	1400
Constant	161.2	161.2	161.2	161.2	161.2
P(0.0105714286)	0	3.70	7.40	11.10	14.80
Yield Strength	161.2	164.9	168.6	172.3	176

Table A9: A1350 Predictor Coefficient Table for Yield Strength

Pressure	0	350	700	1050	1400
Constant	125	125	125	125	125
P(0.0202857143)	0	7.10	14.20	21.30	28.40
Yield Strength	125	132.1	139.2	146.3	153.4

Table A10: Impact Strength of A380 Samples

Injection pressure ($Kg/cm^{2)}$	A380 Sample no	Impact strength (J)	Predicted value
0	1	4.39	4.37
350	2	4.24	4.27
700	3	4.13	4.16
1050	4	4.08	4.06
1400	5	3.93	3.95

Table A11: Impact Strength of A1350 Samples

Injection pressure ($Kg/cm^{2)}$	A1350 Sample no	Impact strength (J)	Predicted value
0	1	4.44	4.42
350	2	4.29	4.31
700	3	4.18	4.20
1050	4	4.09	4.08
1400	5	3.98	3.97

Table A12: Number of Grains for A380 samples

Injection pressure ($Kg/cm^{2)}$	A380 Sample no	Numbers of Grains (g/ mm^2)	Predicted value
0	1	20.31	28.73
350	2	51.56	45.55
700	3	66.63	62.38
1050	4	86.36	79.21
1400	5	87.05	96.04

Table A13: Number of Grains for A1350 samples

Injection pressure ($Kg/cm^{2)}$	A380 Sample no	Numbers of Grains (g/ mm^2)	Predicted value
0	1	20.19	28.02
350	2	50.48	45.44
700	3	67.08	62.86
1050	4	88.02	80.28
1400	5	88.52	97.70

Table A14: Grain sizes for A380 and A1350 samples

Injection pressure ($Kg/cm^{2)}$	A380 Sample no	Grain size (diam/mm)	A1350 Sample no	Grain size (diam/mm)
0	1	11	1	11
350	2	9	2	9
700	3	8	3	8
1050	4	7	4	7
1400	5	6	5	5

Table A15: A380 Predictor Coefficient Table for Grain Size

Pressure	0	350	700	1050	1400
Constant	10.6	10.6	10.6	10.6	10.6
(- 0.00343)P	0	− 1.20	− 2.40	− 3.60	− 4.8
Grain Size	10.6	9.4	8.2	7.0	5.8

Table A16: A1350 Predictor Coefficient Table for Grain Size

Pressure	0	350	700	1050	1400
Constant	10.8	10.8	10.8	10.8	10.8
(- 0.004)P	0	− 1.40	− 2.80	− 4.20	− 5.6
Grain Size	10.8	9.4	8.0	6.6	5.2